JOC The Journal of Organic Chemistry

ARTICLE

pubs.acs.org/joc

# High-Affinity DNA Targeting Using Readily Accessible Mimics of N2′-Functionalized 2′-Amino-α-L-LNA

Saswata Karmakar,[†] Brooke A. Anderson,[†,§] Rie L. Rathje,[†,‡,§] Sanne Andersen,[†,‡,§] Troels B. Jensen,[‡] Poul Nielsen,[‡] and Patrick J. Hrdlicka*[,†]

[†]Department of Chemistry, University of Idaho, Moscow, Idaho 83844, United States

[‡]Nucleic Acid Center, Department of Physics and Chemistry, University of Southern Denmark, 5230 Odense M, Denmark

Supporting Information

**ABSTRACT:** N2′-Pyrene-functionalized 2′-amino-α-L-LNAs (locked nucleic acids) display extraordinary affinity toward complementary DNA targets due to favorable preorganization of the pyrene moieties for hybridization-induced intercalation. Unfortunately, the synthesis of these monomers is challenging (~20 steps, <3% overall yield), which has precluded full characterization of DNA-targeting applications based on these materials. Access to more readily accessible functional mimics would be highly desirable. Here we describe short synthetic routes to a series of O2′-intercalator-functionalized uridine and N2′-intercalator-functionalized 2′-*N*-methyl-2′-aminouridine monomers and demonstrate, via thermal denaturation, UV−vis absorption and fluorescence spectroscopy experiments, that several of them mimic the DNA-hybridization properties of N2′-pyrene-functionalized 2′-amino-α-L-LNAs. For example, oligodeoxyribonucleotides (ONs) modified with 2′-*O*-(coronen-1-yl)methyluridine monomer **Z**, 2′-*O*-(pyren-1-yl)methyluridine monomer **Y**, or 2′-*N*-(pyren-1-ylmethyl)-2′-*N*-methylaminouridine monomer **Q** display prominent increases in thermal affinity toward complementary DNA relative to reference strands (average $\Delta T_m$/mod up to +12 °C), pronounced DNA-selectivity, and higher target specificity than 2′-amino-α-L-LNA benchmark probes. In contrast, ONs modified with 2′-*O*-(2-napthyl)uridine monomer **W**, 2′-*O*-(pyren-1-yl)uridine monomer **X** or 2′-*N*-(pyren-1-ylcarbonyl)-2′-*N*-methylaminouridine monomer **S** display very low affinity toward DNA targets. This demonstrates that even conservative alterations in linker chemistry, linker length, and surface area of the appended intercalators have marked impact on DNA-hybridization characteristics. Straightforward access to high-affinity building blocks such as **Q**, **Y**, and **Z** is likely to accelerate their use in DNA-targeting applications within nucleic acid based diagnostics, therapeutics, and material science.

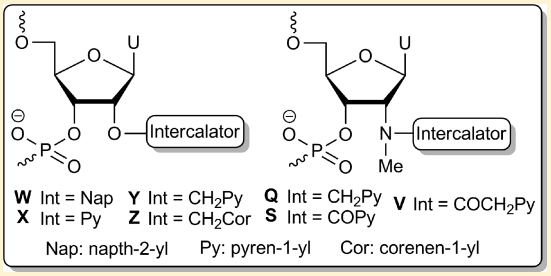


## INTRODUCTION

Development of chemically modified oligonucleotides continues to attract remarkable attention due to their wide-ranging applications within fundamental research, diagnostics, therapeutics, and materials science.[1] Representative applications include modulation of gene expression at the DNA[2] or RNA level,[3] detection of DNA/RNA targets including those with single nucleotide polymorphisms (SNPs),[4] and the use of nucleic acids as supramolecular scaffolds for organization of chromophores.[5]

As part of our ongoing interest in functionalized variants[6] of affinity- and specificity-enhancing LNA (locked nucleic acid)[7] and α-L-LNA,[7c,8] we recently developed oligodeoxyribonucleotides (ONs) modified with N2′-pyrene-functionalized 2′-amino-α-L-LNA monomers.[9] The ability of these monomers to precisely and site-specifically position intercalators in DNA duplex cores results in exceptional affinity toward complementary DNA (cDNA) targets and has enabled us to (a) form dense pyrene arrays within duplex cores,[10] (b) develop probes for fluorescent discrimination of SNPs in DNA targets under nonstringent conditions,[11] and (c) target mixed-sequence regions in double-stranded DNA via the so-called "Invader LNA" approach.[12] The synthesis of the N2′-intercalator-functionalized 2′-amino-α-L-LNA thymine phosphoramidites is unfortunately very challenging. For example, the corresponding phosphoramidite of 2′-*N*-(pyren-1-yl)methyl-2′-amino-α-L-LNA thymine monomer **L** is obtained in ~3% yield over ~20 steps from diacetone-α-D-glucose (Figure 1).[9b,13] Access to synthetically more readily accessible mimics of N2′-intercalator-functionalized 2′-amino-α-L-LNA monomers would be highly desirable to evaluate the full scope of the aforementioned DNA-targeting applications.

We identified O2′-intercalator-functionalized RNA and N2′-intercalator-functionalized 2′-*N*-methyl-2′-amino-DNA monomers (Figure 1) as potential structural and functional mimics of N2′-intercalator-functionalized 2′-amino-α-L-LNA. We based this hypothesis on studies showing (a) that ONs modified with 2′-*O*-(pyren-1-yl)methyluridine monomer **Y** or 2′-*N*-methyl-2′-*N*-(pyren-1-ylmethyl)-2′-amino-DNA monomer **Q** display high thermal affinity toward cDNA,[14,15] and (b) that the pyrene

**Received:** May 28, 2011
**Published:** August 09, 2011

  

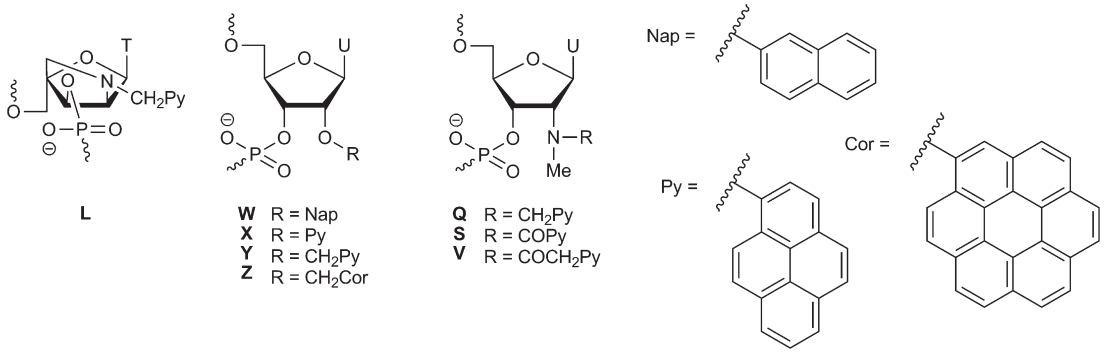


**Figure 1.** Chemical structures of monomers studied herein: 2′-*N*-(pyren-1-yl)methyl-2′-amino-α-L-LNA thymine monomer **L**, O2′-intercalator-functionalized uridine monomers **W**−**Z**, and N2′-intercalator-functionalized 2′-*N*-methyl-2′-aminouridine monomers **Q**, **S**, and **V**.

**Scheme 1. Synthesis of O2′-Intercalator-Functionalized Uridine Phosphoramidites 4W−4Z**

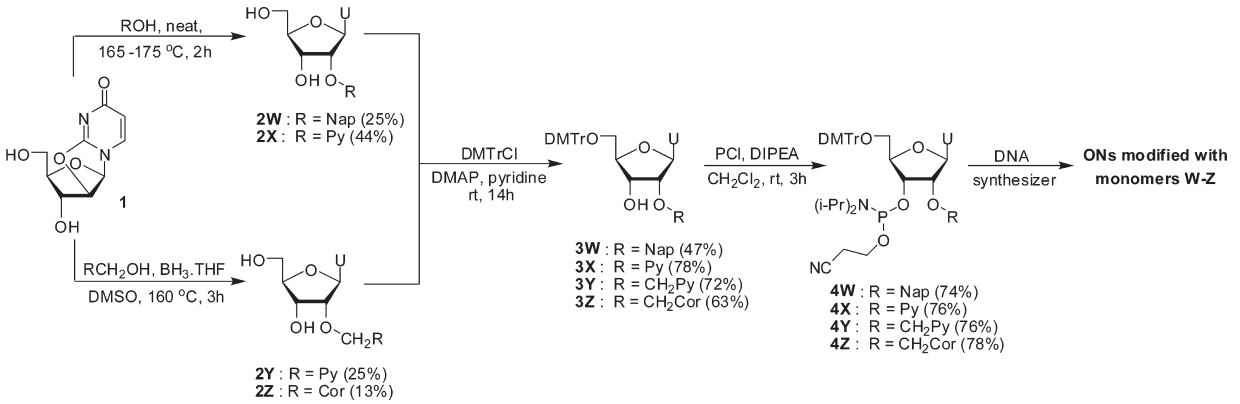


moieties intercalate between the nucleobase of the monomer and the 3′-flanking nucleoside.[16] Motivated by this, we set out to (a) develop synthetic routes to a series of O2′-intercalator-functionalized uridine and N2′-intercalator-functionalized 2′-*N*-methyl-2′-aminouridine phosphoramidites and (b) compare hybridization properties of the correspondingly modified ONs with those of 2′-*N*-(pyren-1-yl)methyl-2′-amino-α-L-LNA "benchmark" probes (Figure 1).

## RESULTS AND DISCUSSION

**Synthesis of O2′-Intercalator-Functionalized Uridine Phosphoramidites.** The four phosphoramidites **4W**−**4Z** were selected as synthetic targets in this series as this allowed us to (a) test whether known monomer **Y**[17] indeed is a mimic of "benchmark" monomer **L** and (b) systematically evaluate the influence of linker length (monomer **X** vs **Y**) and aromatic surface area (monomer **W** vs **X**; monomer **Y** vs **Z**) on the hybridization properties of modified ONs (Scheme 1).

Sekine and co-workers recently described a microwave-based approach in which 2,2′-anhydrouridine **1** is treated with neat phenols to afford O2′-arylated uridines.[18] We adapted this approach for conventional heating sources and used 2-naphtol and 1-pyrenol[19] to obtain **2W**[18] and **2X** in 25% and 44% yield, respectively (Scheme 1). Treatment of **1**[20] with pyren-1-ylmethanol or coronen-1-ylmethanol under similar conditions failed to afford desired products **2Y** and **2Z** in acceptable yields, requiring development of an alternative approach.

Yamana and co-workers previously installed arylmethyl groups at the O2′-position of 3′,5′-ditrityluridine via Williamson etherification.[17,21] We found the initial O3′,O5′-tritylation of uridine[22] and the protecting group manipulations following the O2′-functionalization step to be cumbersome. Instead, the reaction between **1** and tris(pyrene-1-ylmethyl) or tris(coronene-1-ylmethyl) borate, generated in situ upon addition of pyren-1-ylmethanol[23] or coronen-1-ylmethanol[24] to borane, afforded **2Y** and **2Z** in modest but robust yields (Scheme 1).[25] The two-step route to nucleoside **2Y** from uridine proceeds in similar yield (∼20%) as the original three-step approach[17] but is more convenient. To our knowledge, this is the first time that the trialkyl borate mediated opening[26] of O2,O2′-anhydrouridine **1** has been used to install large arylmethylethers at the C2′-position of nucleosides. Subsequent O5′-dimethoxytritylation afforded nucleosides **3W**−**3Z** in 47−78% yield, which upon treatment with 2-cyanoethyl-*N*,*N*-diisopropylchlorophosporamidite (PCl reagent) and Hünig's base provided target phosphoramidites **4W**−**4Z** in 74−78% yield (Scheme 1).

**Synthesis of N2′-Pyrene-Functionalized 2′-*N*-Methyl-2′-aminodeoxyuridine Phosphoramidites.** In this series, three phosphoramidites **7Q**, **7S**, and **7V** were selected as synthetic targets to (a) evaluate whether known monomer **Q**[15] is a mimic of benchmark monomer **L** and (b) to study the influence of linker chemistry (monomer **Q** vs **S**) and length (monomer **S** vs **V**) on hybridization properties of correspondingly modified ONs (Scheme 2).

Wengel and co-workers previously reported a route to 2′-*N*-methyl-2′-*N*-(pyren-1-ylmethyl)-2′-aminouridine phosphoramidite


dx.doi.org/10.1021/jo201095p |*J. Org. Chem.* 2011, 76, 7119–7131

**Scheme 2. Synthesis of N2′-Intercalator-Functionalized Uridine Phosphoramidites 7Q, 7S, and 7V**

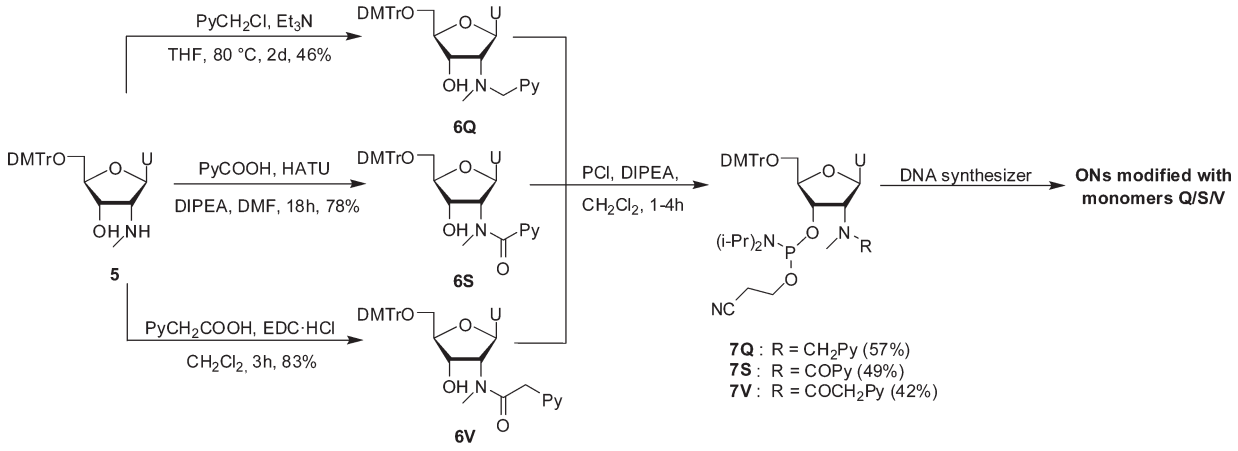


**7Q** from 5′-*O*-dimethoxytrityl-2′-aminouridine, which entails N2′-functionalization via reductive amination, O5′-detritylation, N2′-methylation under acidic conditions, O5′-tritylation, and O3′-phophitylation (~7% overall yield over five steps).[15] In order to decrease the number of protection/deprotection steps and to introduce N2′-moieties at a later stage, we instead decided to utilize nucleoside **5** as a starting material, which is easily obtained from 5′-*O*-dimethoxytrityl-2,2′-anhydrouridine in ~73% yield over three steps.[27] Direct N2′-alkylation of **5** using pyren-1-ylmethyl chloride afforded the desired product **6Q** in 46% yield.[25] Interestingly, reductive amination of **5** using 1-pyrenecarbaldehyde and sodium triacetoxyborohydride[28] or sodium cyanoborohydride failed to afford **6Q** in acceptable yields due to prominent formation of the corresponding cyclic N2′,O3′-hemiaminal ether (see Supporting Information, Scheme S1). Although formation of this byproduct was avoided by prior protection of the O3′-position of **5** as a TBDMS-ether, the increased steric bulk resulted in low yields during the subsequent reductive amination (results not shown).

HATU-mediated coupling between nucleoside **5** and 1-pyrenecarboxylic acid afforded N2′-acylated nucleoside **6S** in 78% yield, while EDC-mediated coupling between nucleoside **5** and 1-pyreneacetic acid furnished **6V** in 83% yield.[25] Subsequent O3′-phosphitylation of **6Q**, **6S**, and **6V** using similar conditions as for the synthesis of **4W**−**4Z** afforded phosphoramidites **7Q**, **7S**, and **7V** although only in moderate yields (42−57%), presumably due to the increased steric bulk at the N2′-position.

**Synthesis of Modified ONs and Setup of Thermal Denaturation Studies.** Intercalator-functionalized phosphoramidites **4W**, **4X**, **4Y**, **4Z**, **7Q**, **7S**, and **7V** were incorporated into ONs via machine-assisted solid-phase DNA synthesis using the following hand-coupling conditions (activator; coupling time; approximate coupling yield): monomer **W**/**X**/**Y** (4,5-dicyanoimidazole; 15 min; ~98%/~98%/~98%); monomer **Z** (4,5-dicyanoimidazole; 35 min; ~90%); monomers **Q**, **S**, and **V** (5-(bis-3,5-trifluoromethylphenyl)-1*H*-tetrazole [Activator 42]; 15 min; ~95%/~89%/~99%). Suitable activators were identified through initial screening of common activators (results not discussed). The studied 9-mer sequences have been previously used to study ONs modified with 2′-*N*-(pyren-1-yl)-methyl-2′-amino-α-L-LNA thymine monomer **L**.[9b] ONs containing a single incorporation in the 5′-GBG ATA TGC context are denoted **V1**, **W1**, **Y1**, **Z1**, **Q1**, **S1**, **V1** and **L1**, respectively. Similar conventions apply for ONs in the **B2**−**B7** series (Table 1). In addition, the following descriptive nomenclature is used: O2′-Nap (**W** series), O2′-Py (**X** series), O2′-PyMe (**Y** series), O2′-CorMe (**Z** series), N2′-PyMe (**Q** series), N2′-PyCO (**S** series), N2′-PyAc (**V** series), and N2′-PyMe-α-L-LNA (**L** series). Reference DNA and RNA strands are denoted **D1**/**D2** and **R1**/**R2**, respectively.

The thermal affinity of **B1**−**B7** toward cDNA or cRNA targets was evaluated via UV thermal denaturation experiments using a medium salt buffer that mimics physiological ionic strengths ([$Na^+$] = 110 mM, Tables 1 and 2). As expected, all denaturation curves display monophasic sigmoidal transitions (Figures S1 and S2 in Supporting Information). Changes in thermal denaturation temperatures ($T_m$ values) of modified duplexes are discussed relative to $T_m$ values of unmodified reference duplexes, unless otherwise mentioned. The effect on duplex thermostability upon exchanging thymine moieties (reference ONs) with uracil moieties (modified ONs) is recognized ($\Delta T_m$/modification [$\Delta T_m$/mod] ≈ −0.5 °C)[29] but otherwise disregarded.

**Thermal Affinity toward Complementary DNA/RNA; O2′-Intercalator-Functionalized Uridine Monomers W**−**Z.** The effects on thermal DNA affinity upon incorporation of O2′-functionalized uridine monomers **W**−**Z** into ONs vary dramatically ($\Delta T_m$/mod = −13.0 to +20.0 °C, Table 1). The observed trends in DNA affinity of singly modified ONs (**Z** ≥ **L** > **Y** ≫ **X** ≫ **V**) suggest that (a) 2′-*O*-(pyren-1-yl)methyluridine monomer **Y** is a mimic of 2′-*N*-(pyren-1-yl)methyl-2′-amino-α-L-LNA benchmark monomer **L** with respect to DNA-hybridization properties and binding mode, albeit slightly lower duplex thermostabilization is observed ($\Delta T_m$/mod = +3.5 to +12.5 °C vs +6.5 to +15.5 °C, for **Y1**−**Y5** and **L1**−**L5**, respectively, Table 1); (b) increasing the intercalator surface area leads to additional stabilization of DNA duplexes (O2′-PyMe monomer **Y** → O2′-CorMe monomer **Z**, $\Delta T_m$/mod = +4.5 to +20.0 °C, Table 1); (c) shortening the linker between the furanose and pyrene moiety by one $CH_2$-group results in markedly lower thermal affinity toward cDNA (O2′-PyMe monomer **Y** → O2′-Py monomer **X**, $\Delta T_m$/mod = −3.5 to +4.0 °C, Table 1); and (d) concomitant reduction in aromatic surface area results in additionally decreased DNA duplex thermostability (O2′-Py monomer **X** → O2′-Nap monomer **W**, $\Delta T_m$/mod = −13.0 to −5.0 °C, Table 1). The results underline that intercalation is an important binding mode for monomers **Y** and **Z** and corroborate earlier studies demonstrating that pyrene and coronene


dx.doi.org/10.1021/jo201095p |*J. Org. Chem.* 2011, 76, 7119–7131

Table 1. $T_m$ Values of Duplexes between B1−B7 and Complementary DNA Targets[a]

| | | | $T_m$ [$\Delta T_m$/mod] (°C) | | | | | | | | |
|---|---|---|---|---|---|---|---|---|---|---|---|
| ON | duplex | B = | T | W | X | Y | Z | Q | S | V | L[9b] |
| **B1** | 5′-GBG ATA TGC | | 29.5 | 21.5 [−8.0] | 26.5 [−3.0] | 34.5 [+5.0] | 34.0 [+4.5] | 34.5 [+5.0] | 23.5 [−6.0] | 29.0 [−0.5] | 36.5 [+7.0] |
| **D2** | 3′-CAC TAT ACG | | | | | | | | | | |
| **B2** | 5′-GTG ABA TGC | | 29.5 | 24.5 [−5.0] | 33.5 [+4.0] | 42.0 [+12.5] | 49.5 [+20.0] | 43.5 [+14.0] | 32.5 [+3.0] | 35.5 [+6.0] | 43.5 [+14.0] |
| **D2** | 3′-CAC TAT ACG | | | | | | | | | | |
| **B3** | 5′-GTG ATA BGC | | 29.5 | 24.5 [−5.0] | 26.0 [−3.5] | 37.5 [+8.0] | 40.5 [+11.0] | ND | ND | ND | 40.0 [+10.5] |
| **D2** | 3′-CAC TAT ACG | | | | | | | | | | |
| **D1** | 5′-GTG ATA TGC | | 29.5 | 16.5 [−13.0] | 26.0 [−3.5] | 33.0 [+3.5] | 36.0 [+6.5] | 31.0 [+1.5] | 23.5 [−6.0] | 30.5 [+1.0] | 36.0 [+6.5] |
| **B4** | 3′-CAC BAT ACG | | | | | | | | | | |
| **D1** | 5′-GTG ATA TGC | | 29.5 | 24.5 [−5.0] | 30.5 [+1.0] | 41.0 [+11.5] | 45.5 [+16.0] | 42.5 [+13.0] | 33.5 [+4.0] | 36.0 [+6.5] | 45.0 [+15.5] |
| **B5** | 3′-CAC TAB ACG | | | | | | | | | | |
| **D1** | 5′-GTG ATA TGC | | 29.5 | ND | 25.5 [−2.0] | 43.5 [+7.0] | 47.0 [+8.8] | 43.5 [+7.0] | ND | 37.0 [+3.8] | ND |
| **B6** | 3′-CAC BAB ACG | | | | | | | | | | |
| **B7** | 5′-GBG ABA BGC | | 29.5 | ND | 25.5 [−1.3] | 51.0 [+7.2] | ND | ND | ND | ND | ND |
| **D2** | 3′-CAC TAT ACG | | | | | | | | | | |

[a] $\Delta T_m$ = change in $T_m$'s relative to unmodified reference duplex; $T_m$'s determined as the maximum of the first derivative of melting curves ($A_{260}$ vs $T$) recorded in medium salt buffer ([$Na^+$] = 110 mM, [$Cl^-$] = 100 mM, pH 7.0 ($NaH_2PO_4/Na_2HPO_4$)), using 1.0 $\mu$M of each strand. $T_m$'s are averages of at least two measurements within 1.0 °C; **A** = adenin-9-yl DNA monomer, **C** = cytosin-1-yl DNA monomer, **G** = guanin-9-yl DNA monomer, **T** = thymin-1-yl DNA monomer. ND = not determined. For structures of monomers **Q**−**Z** see Figure 1.

moieties engage in efficient $\pi-\pi$ stacking with flanking nucleobases.[16,30,31] The shorter linker of monomers **W** and **X**, in contrast, seems to render intercalative binding modes less likely. The magnitude of DNA duplex thermostabilization is highly sequence-dependent, in particular for ONs modified with monomer **Z**. Particularly pronounced stabilization is observed when **Z** is centrally incorporated and flanked by purines (e.g., compare $\Delta T_m$/mod values for **Z2** and **Z4**). This reflects strong $\pi-\pi$ stacking efficiency with large 3′-flanking purines.[9b,14]

Singly modified ONs **B1**−**B5** display similar relative trends in thermal affinity toward cRNA (**Z** ≈ **L** > **Y** ≫ **X** > **W**) as toward cDNA except that the resulting duplexes are considerably less stable ($\Delta T_m$/mod = −12.0 to +10.5 °C, Table 2). In fact, none of the monomers consistently induces increased thermal affinity relative to reference strand **D1**. Substantial DNA-selectivity, defined as $\Delta\Delta T_m$ (DNA-RNA) = $\Delta T_m$ (vs DNA) − $\Delta T_m$ (vs RNA) > 0 °C, is therefore observed (Table 3). The DNA-selectivity of O2′-$CH_2$Py-modified **Y1**−**Y5** and O2′-$CH_2$Cor-modified **Z1**−**Z5** is especially pronounced and comparable to that of the corresponding N2′-PyMe-α-L-LNA **L1**−**L5** (Table 3). The extensive DNA-selectivity of doubly O2′-$CH_2$Cor-modified **Z6** is particularly noteworthy and hints at interesting DNA-targeting applications for multilabeled ONs ($\Delta\Delta T_m$ (DNA-RNA) = 31.0 °C, Table 3). DNA-selective hybridization is typically observed for ONs modified with intercalating moieties,[9b,14,32,33] since intercalation favors the less compressed B-type helix geometry of DNA:DNA duplexes. In contrast, most of the O2′-Py-modified **X**-series and all O2′-Nap-modified **W1**−**W5**, in particular, display much lower DNA-selectivity, indicating that intercalative binding modes are less prominent with these monomers than with **Y** and **Z** monomers (Table 3).

**Thermal Affinity toward Complementary DNA/RNA; N2′-Pyrene-Functionalized 2′-*N*-Methyl-2′-aminodeoxyuridine Monomers Q, S, and V.** The highly variable effects on thermal affinity toward DNA targets upon incorporation of N2′-pyrene-functionalized 2′-*N*-methyl-2′-aminodeoxyuridine monomers **Q**, **S**, and **V** into ONs are intriguing considering the very conservative differences in linker chemistry and linker length ($\Delta T_m$/mod = −6.0 to +14.0 °C, Table 1). The observed trends in DNA duplex thermostabilization of singly modified ONs (**L** > **Q** ≫ **V** > **S**) suggest that (a) 2′-*N*-(pyren-1-ylmethyl)-2′-*N*-methylaminouridine monomer **Q** indeed is a mimic of N2′-PyMe-α-L-LNA monomer **L** with respect to DNA-hybridization properties and binding mode ($\Delta T_m$/mod = +1.5 to +14.0 °C, Table 1); (b) monomers where the pyrene moiety is attached via N2′-alkyl linkers are preferred over those with N2′-alkanoyl linkers (compare $\Delta T_m$/mod for **S1**−**S5** = −6.0 to +4.0 °C with data for **Q1**−**Q5**, Table 1); and (c) extending the N2′-alkanoyl linker between the furanose and pyrene moiety as in ONs modified with 2′-*N*-(pyren-1-ylmethycarbonyl)-2′-aminouridine monomer **V**, partially reverses the detrimental effects of N2′-acylation on DNA duplex thermostability (N2′-PyCO monomer **S** → N2′-PyAc monomer **V**, $\Delta T_m$/mod = −0.5 to +6.5 °C, Table 1). ONs with central incorporations of N2′-acylated 2′-*N*-aminouridine monomers (i.e., without the 2′-*N*-methyl group of monomers **Q**, **S**, and **V**) are known to display low affinity toward DNA targets.[34,35] This suggests that the low thermal affinity observed for ONs in the **S** and **V** series is a consequence of the 2′-*N*-amido substituent rather than the "extra" 2′-*N*-methyl group. We speculate that the rigid 2′-*N*-alkanoyl linker positions the intercalator in a position less favorable for affinity-enhancing intercalation and/or that increased solvation of the linker stabilizes the single-stranded state rendering hybridization less energetically favorable.

**Table 2. $T_m$ Values of Duplexes between B1−B7 and Complementary RNA Targets[a]**

| | | | $T_m$ [$\Delta T_m$/mod] (°C) | | | | | | | | |
|---|---|---|---|---|---|---|---|---|---|---|---|
| ON | duplex | B = | T | W | X | Y | Z | Q | S | V | $L^{9b}$ |
| **B1** | 5′-G**B**G ATA TGC | | 26.5 | 21.0 [−5.5] | 22.5 [−4.0] | 24.5 [−2.0] | 21.5 [−5.0] | 22.0 [−4.5] | 14.0 [−12.5] | 20.0 [−6.5] | 27.0 [+0.5] |
| **R2** | 3′-CAC UAU ACG | | | | | | | | | | |
| **B2** | 5′-GTG A**B**A TGC | | 26.5 | 16.0 [−10.5] | 22.5 [−4.0] | 30.5 [+4.0] | 37.0 [+10.5] | 29.0 [+2.5] | 18.0 [−8.5] | 28.0 [+1.5] | 31.5 [+5.0] |
| **R2** | 3′-CAC UAU ACG | | | | | | | | | | |
| **B3** | 5′-GTG ATA **B**GC | | 26.5 | 18.0 [−8.5] | 14.5 [−12.0] | 26.5 [±0.0] | 30.5 [+4.0] | ND | ND | ND | 28.0 [+1.5] |
| **R2** | 3′-CAC UAU ACG | | | | | | | | | | |
| **R1** | 5′-GUG AUA UGC | | 24.5 | 16.5 [−8.0] | 16.5 [−8.0] | 20.0 [−4.5] | 22.5 [−2.0] | 17.5 [−7.0] | 9.0 [−15.5] | 16.0 [−8.5] | 23.5 [−1.0] |
| **B4** | 3′-CAC **B**AT ACG | | | | | | | | | | |
| **R1** | 5′-GUG AUA UGC | | 24.5 | 19.5 [−5.0] | 21.5 [−3.0] | 27.0 [+2.5] | 30.5 [+6.0] | 27.0 [+2.5] | 16.0 [−8.5] | 26.5 [+2.0] | 32.0 [+7.5] |
| **B5** | 3′-CAC TA**B** ACG | | | | | | | | | | |
| **R1** | 5′-GUG AUA UGC | | 24.5 | ND | 14.5 [−5.0] | 24.0 [−0.3] | 11.0 [−6.8] | 20.0 [−2.3] | ND | 19.0 [−2.8] | ND |
| **B6** | 3′-CAC **B**A**B** ACG | | | | | | | | | | |
| **B7** | 5′-G**B**G A**B**A **B**GC | | 26.5 | ND | 15.5 [−3.7] | 27.5 [+0.3] | ND | ND | ND | ND | ND |
| **D2** | 3′-CAC UAU ACG | | | | | | | | | | |

[a] For conditions of thermal denaturation experiments, see Table 1.

**Table 3. DNA-Selectivity of B1−B7[a]**

| | | $\Delta\Delta T_m$ (DNA-RNA) [°C] | | | | | | | |
|---|---|---|---|---|---|---|---|---|---|
| ON | sequence B = | W | X | Y | Z | Q | S | V | $L^{9b}$ |
| **B1** | 5′-G**B**G ATA TGC | −2.5 | +1.0 | +7.0 | +9.5 | +9.5 | +6.5 | +6.0 | +6.5 |
| **B2** | 5′-GTG A**B**A TGC | +5.5 | +8.0 | +8.5 | +9.5 | +11.5 | +11.5 | +4.5 | +9.0 |
| **B3** | 5′-GTG ATA **B**GC | +3.5 | +8.5 | +8.0 | +7.0 | ND | ND | ND | +9.0 |
| **B4** | 3′-CAC **B**AT ACG | +5.0 | +4.5 | +8.0 | +8.5 | +8.5 | +9.5 | +9.5 | +7.5 |
| **B5** | 3′-CAC TA**B** ACG | 0 | +4.0 | +9.0 | +10.0 | +10.5 | +12.5 | +4.5 | +8.0 |
| **B6** | 3′-CAC **B**A**B** ACG | ND | +6.0 | +14.5 | +31.0 | +18.5 | ND | +13.0 | ND |
| **B7** | 5′-G**B**G A**B**A **B**GC | ND | +7.0 | +20.5 | ND | ND | ND | ND | ND |

[a] DNA-selectivity defined as $\Delta\Delta T_m$ (DNA-RNA) = $\Delta T_m$ (vs DNA) − $\Delta T_m$ (vs RNA).

The hybridization characteristics of ONs modified with monomers **Q**/**S**/**V** share several points of similarity with ONs modified with monomers **W**−**Z**: (a) thermostabilization of DNA duplexes is highly sequence-dependent; (b) incorporation of two monomers as next-nearest neighbors leads to additive increases in DNA duplex thermostability (i.e., compare $\Delta T_m$/mod values for **Q4**−**Q6**, Table 1); (c) duplexes with complementary RNA are dramatically destabilized ($\Delta T_m$/mod = −15.5 to +2.5 °C, Table 2); and (d) extensive DNA-selectivity is observed which is most pronounced for N2′-PyMe-modified **Q1**−**Q5** and N2′-PyCO-modified **S1**−**S5** ($\Delta\Delta T_m$ (DNA-RNA) up to +12.5 °C, Table 3). The latter is in agreement with the suggested intercalative pyrene binding mode for monomer **Q**[15] while the pronounced DNA-selectivity of **S1**−**S5** is more surprising given the low DNA duplex thermostability. This indicates that intercalation of the pyrene moiety remains an important binding mode for monomer **S** but that it interferes with duplex formation. The less pronounced DNA-selectivity of **V1**−**V6** seems to suggest that intercalative pyrene binding modes are less dominant for monomer **V**.

To sum up, the thermal denaturation data suggest that O2′-PyMe monomer **Y**, O2′-CorMe monomer **Z**, and N2′-PyMe monomer **Q** are mimics of N2′-PyMe-α-L-LNA monomer **L** and attractive candidates for DNA targeting applications.

**Mismatch Discrimination.** The Watson−Crick specificity of singly modified ONs (**B2** series) was evaluated using DNA (Table 4) or RNA targets (Table S4 in Supporting Information) with mismatched nucleotides opposite of the incorporation site. ONs in the **B2** series generally display reduced DNA target specificity relative to reference strand **D1**, which is in agreement with observations on other intercalator-functionalized ONs.[9b,36,37] For example, O2′-PyMe-modified **Y2** and O2′-CorMe-modified **Z2** discriminate dT-mismatches very poorly relative to **D1** (compare $\Delta T_m$ values for **D1**, **Y2**, and **Z2** against targets with a dT-mismatch, Table 4), while dC- and dG-mismatches almost are as efficiently discriminated as with **D1**. N2′-PyMe-α-L-LNA **L2** has a similar specificity profile but discriminates the dT-mismatch even more poorly. Interestingly, N2′-PyMe-modified **Q2** displays substantially better discrimination of dC- and dT-mismatches than **Y2**, **Z2**, and **L2** rendering it as the most specific of the high-affinity DNA-targeting modifications. Even minor changes in linker chemistry and length have marked influence on target specificity. Thus, N2′-PyCO-modified **S2** displays similar DNA target specificity as **Y2**, **Z2**, and **L2**, while N2′-PyAc-modified **V2** discriminates DNA mismatches more poorly. Similarly, O2′-Nap-modified **W2** exhibits very poor target specificity, while O2′-Py-modified **X2** displays much higher target specificity than **W2** or O2′-PyMe-modified **Y2** (Table 4). Structural models (e.g., NMR solution structures) will be necessary to fully understand the molecular underpinnings of these trends.


dx.doi.org/10.1021/jo201095p |J. Org. Chem. 2011, 76, 7119–7131

**Table 4. Discrimination of Mismatched DNA Targets by B2 Series and Reference Strands[a]**

| | | | DNA: 3′-CAC TBT ACG | | | |
|---|---|---|---|---|---|---|
| | | | $T_m$ [°C] | $\Delta T_m$ [°C] | | |
| ON | sequence | B = | A | C | G | T |
| **D1** | 5′-GTG ATA TGC | | **29.5** | −16.5 | −9.5 | −17.0 |
| **W2** | 5′-GTG AWA TGC | | **24.5** | −11.0 | +2.0 | −3.5 |
| **X2** | 5′-GTG AXA TGC | | **33.5** | −23.5 | −7.0 | −13.0 |
| **Y2** | 5′-GTG AYA TGC | | **42.0** | −13.0 | −5.0 | −6.5 |
| **Z2** | 5′-GTG AZA TGC | | **49.0** | −13.5 | −6.0 | −7.0 |
| **Q2** | 5′-GTG AQA TGC | | **43.5** | −22.0 | −3.5 | −12.0 |
| **S2** | 5′-GTG ASA TGC | | **32.5** | −11.5 | −9.0 | −8.5 |
| **V2** | 5′-GTG AVA TGC | | **35.5** | −11.5 | +1.5 | −3.5 |
| **L2**[9b] | 5′-GTG ALA TGC | | **43.5** | −12.5 | −5.5 | −3.5 |

[a] For conditions of thermal denaturation experiments, see Table 1. $T_m$ values of fully matched duplexes are shown in bold. $\Delta T_m$ = change in $T_m$ relative to fully matched DNA:DNA duplex.

**Table 5. Discrimination of Mismatched DNA Targets by B6 Series and Reference Strands[a]**

| | | | DNA: 5′-GTG ABA ACG | | | |
|---|---|---|---|---|---|---|
| | | | $T_m$ [°C] | $\Delta T_m$ [°C] | | |
| ON | sequence | B = | T | A | C | G |
| **D2** | 3′-CAC TAT ACG | | **29.5** | −17.0 | −15.5 | −9.0 |
| **X6** | 3′-CAC XAX ACG | | **25.5** | −15.5 | −14.0 | −14.5 |
| **Y6** | 3′-CAC YAY ACG | | **43.5** | −24.0 | −17.0 | −14.0 |
| **Z6** | 3′-CAC ZAZ ACG | | **47.0** | −19.5 | −13.0 | −11.0 |
| **Q6** | 3′-CAC QAQ ACG | | **43.5** | −21.5 | −10.5 | −13.5 |
| **V6** | 3′-CAC VAV ACG | | **37.0** | −14.5 | −13.5 | −11.0 |

[a] For conditions of thermal denaturation experiments, see Table 1. $T_m$ values of fully matched duplexes are shown in bold. $\Delta T_m$ = change in $T_m$ relative to fully matched DNA:DNA duplex.

The specificity of ONs with two modifications positioned as next-nearest neighbors (**B6** series) was evaluated against DNA targets with a single central mismatched nucleotide opposite the central 2′-deoxyadenosine residue (Table 5). This probe design generally results in improved mismatch discrimination relative to reference strand **D2** with specificity decreasing in the following manner: **Y6** > **X6** > **Z6** ≈ **Q6** > **V6**; A- and G-mismatches are particularly efficiently discriminated. Subsequent experiments will reveal if these "intercalator-capped fidelity cassettes" can be used as general motifs to develop ONs with improved target specificity.

**Optical Spectroscopy.** Absorption and steady state fluorescence emission spectra of ONs modified with monomers **Q**, **S**, **V**, **X**, and **Y** in the presence or absence of cDNA/cRNA targets were recorded to gain additional insight into the binding modes of the pyrene moieties. Intercalation of pyrene moieties is known to induce bathochromic shifts of pyrene absorption peaks.[38] In agreement with this, ONs modified with monomers **Q**, **S**, **V**, and **Y** display significant bathochromic shifts upon hybridization with DNA targets (average $\Delta\lambda_{max}$ = 2.8−5.0 nm, respectively, Table 6; see also Figure S4 and Tables S5 and S6 in Supporting Information). Hybridization with cRNA leads to slightly smaller bathochromic shifts as intercalation into increasingly compressed A-type duplexes is less favorable (average $\Delta\lambda_{max}$ = 2.0−4.5 nm, Table 6). O2′-Py-modified **X1**−**X5** display distinctly smaller hybridization-induced bathochromic shifts than the other pyrene-functionalized ONs (average $\Delta\lambda_{max}$ ∼0.6 nm, Table 6), which substantiates the trends from thermal denaturation studies suggesting that intercalation of the pyrene moiety is a less important binding mode for monomer **X**.

The steady-state fluorescence emission spectra ($\lambda_{ex}$ = 350 nm; $\lambda_{em}$ = 360−600 nm; $T$ = 5 °C) display the two expected vibronic bands I and III at $\lambda_{em}$ = 382 ± 3 and 402 ± 3 nm, respectively, as well as a small shoulder at ∼420 nm (Figure 2). Hybridization of ONs modified with monomers **Q**, **S**, **V**, **X**, or **Y** with cRNA, and cDNA in particular, results in reduced fluorescence emission intensity (see Figure 2 for **B4** series; see Figures S5−S9 in Supporting Information for all series). This trend corroborates pyrene intercalation as nucleobase moieties are known to quench pyrene fluorescence via photoinduced electron transfer (PET) with guanine and cytosine moieties being the strongest quenchers.[39] In agreement with this, duplexes involving the **Y**, **Q**, and **V** series (intercalation is important binding mode) display far lower emission intensity than those involving the **X** series (intercalation is less important binding mode). Sequence-specific deviations from general trends are observed in some cases (e.g., **Q2**, **S1**, **S4**, and **S5**, see Figures S7−S8 in Supporting Information), which likely reflects a trend-defying duplex geometry or positioning of the pyrene moiety. For additional discussion of fluorescence emission data, please see the Supporting Information.

On balance, the data from the thermal denaturation and optical spectroscopy studies (DNA-selectivity; mismatch discrimination; UV−vis; fluorescence) suggest that intercalation of the attached hydrocarbon is a possible binding mode for all studied monomers. Intercalation is least important for monomers **W** and **X**, while being a dominant binding mode for monomers **Y**, **Z**, and **Q**.

**Table 6. Average Bathochromic Shifts of Pyrene Absorption Bands ($\lambda_{em}$ ∼350 nm) upon Hybridization of Pyrene-Functionalized ONs with Complementary DNA/RNA Targets[a]**

| | average $\Delta\lambda_{max}$ (nm) | | | | | | | | | | | |
|---|---|---|---|---|---|---|---|---|---|---|---|---|
| B = | X | | Y | | Q | | S | | V | | L[9b] | |
| | +DNA | +RNA | +DNA | +RNA | +DNA | +RNA | +DNA | +RNA | +DNA | +RNA | +DNA | +RNA |
| | 0.6 ± 1.8 | 0.6 ± 1.3 | 3.4 ± 1.1 | 2.6 ± 0.9 | 5.0 ± 0.8 | 2.3 ± 1.7 | 2.8 ± 1.0 | 2.0 ± 1.8 | 4.5 ± 0.6 | 4.5 ± 1.3 | 2.5 ± 1.0 | 1.0 ± 0.8 |

[a] Values are averages of measurements performed for **B1**−**B5** at 5 °C (**Q**, **S**, **V**), 7 °C (**X**, **Y**), or room temperature (**L**).[9b] Buffer conditions are as for thermal denaturation experiments. ± denotes standard deviation. For full data set, see Tables S5 and S6 in Supporting Information.


dx.doi.org/10.1021/jo201095p |J. Org. Chem. 2011, 76, 7119–7131

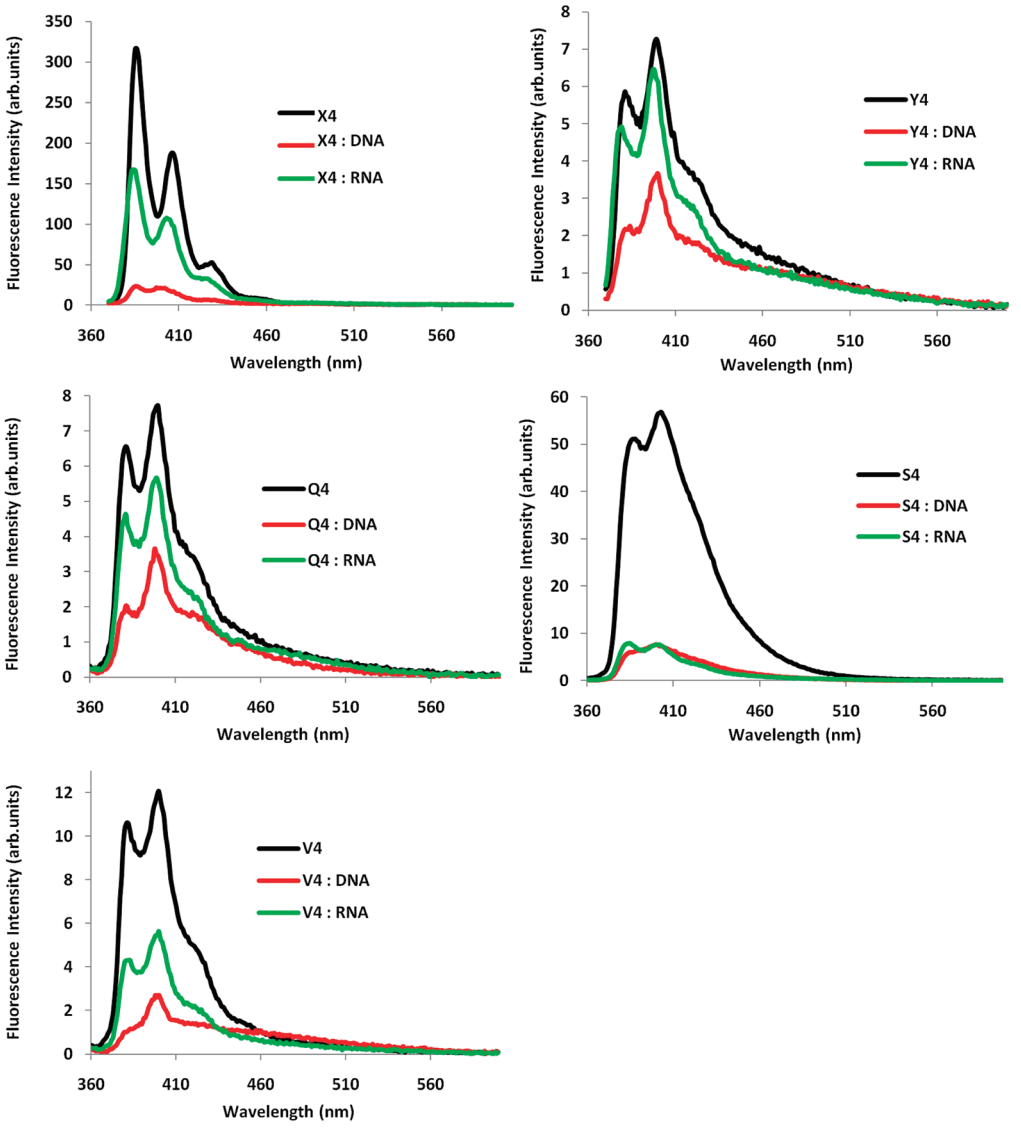


**Figure 2.** Fluorescence emission spectra of **B4** series in the presence or absence of cDNA/RNA ($\lambda_{ex}$ = 350 nm; $T$ = 5 °C; [ON] = 1.0 $\mu$M). Note that different *y*-axes are used.

## CONCLUSION

We have developed short routes to a series of O2′-intercalator-functionalized uridine and N2′-intercalator-functionalized 2′-*N*-methyl-2′-aminouridine phosphoramidites. Thermal denaturation studies of correspondingly modified ONs reveal that even very conservative changes in linker chemistry, linker length, or surface area of the intercalator translate into markedly different DNA-hybridization characteristics (Figure 3). We propose the following guidelines for design of high-affinity DNA-targeting monomers based on uridine or 2′-*N*-methyl-2′-aminouridine scaffolds: (a) direct attachment of intercalators to the O2′-position of uridine should be avoided (e.g., monomer **W** and **X**), (b) attachment of intercalators to the N2′-position of 2-*N*-methyl-2′-aminouridine via alkanoyl linkers should be avoided (e.g., monomer **S** and **V**), and (c) attachment of large intercalators via a methylene linker is desirable (e.g., monomers **Q**, **Y**, and **Z**). Thus, ONs modified with 2′-*O*-(pyren-1-yl)-methyluridine monomer **Y**, 2′-*O*-(coronen-1-yl)methyluridine

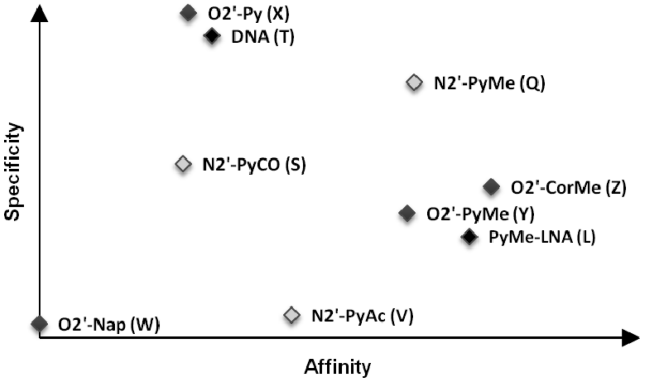


**Figure 3.** Qualitative representation of DNA-hybridization characteristics of O2′-intercalator-functionalized uridine (light gray) and N2′-intercalator-functionalized 2′-*N*-methyl-2′-aminouridine (dark gray) monomers studied herein relative to reference monomers **L** and **T** (black).


dx.doi.org/10.1021/jo201095p |*J. Org. Chem.* 2011, 76, 7119–7131

monomer **Z**, or 2′-*N*-(pyren-1-ylmethyl)-2′-*N*-methylaminouridine monomer **Q** display similar thermal affinity toward DNA complements (average $\Delta T_m$/mod between +8 and +12 °C) and higher target specificity than ONs modified with 2′-*N*-(pyren-1-yl)-methyl-2′-amino-α-L-LNA benchmark monomer **L** (Figure 3). The highly DNA-selective hybridization of these ONs, and of the doubly O2′-$CH_2$Cor-modified **Z6** in particular ($\Delta\Delta T_m$ (DNA-RNA) = 31.0 °C), hints at interesting applications within DNA diagnostics. Straightforward access to these monomers will likely spur their use within nucleic acid based diagnostics, therapeutics, and material science.[10−12,40−42] Studies along these lines are ongoing and will be reported shortly.

## EXPERIMENTAL SECTION

**General Experimental Section.** Unless otherwise noted, reagents and solvents were commercially available, of analytical grade, and used without further purification. Petroleum ether of the distillation range 60−80 °C was used. Solvents were dried over activated molecular sieves: acetonitrile and THF (3 Å); $CH_2Cl_2$, 1,2-dichloroethane, *N*,*N*′-diisopropylethylamine, and anhydrous DMSO (4 Å). Water content of "anhydrous" solvents was verified on Karl Fischer apparatus. Reactions were conducted under argon whenever anhydrous solvents were used. Reactions were monitored by TLC using silica gel coated plates with a fluorescence indicator ($SiO_2$-60, F-254) which were visualized (a) under UV light and/or (b) by dipping in 5% conc $H_2SO_4$ in absolute ethanol (v/v) followed by heating. Silica gel column chromatography was performed with silica gel 60 (particle size 0.040−0.063 mm) using moderate pressure (pressure ball). Evaporation of solvents was carried out under reduced pressure at temperatures below 45 °C. After column chromatography, appropriate fractions were pooled, evaporated, and dried at high vacuum for at least 12 h to give the obtained products in high purity (>95%) as ascertained by 1D NMR techniques. Chemical shifts of $^1$H NMR (500 MHz), $^{13}$C NMR (125.6 MHz), and/or $^{31}$P NMR (121.5 MHz) are reported relative to deuterated solvent or other internal standards (80% phosphoric acid for $^{31}$P NMR). Exchangeable (ex) protons were detected by disappearance of signals upon $D_2O$ addition. Assignments of NMR spectra are based on 2D spectra (HSQC, COSY) and DEPT spectra. Quaternary carbons are not assigned in $^{13}$C NMR but verified from HSQC and DEPT spectra (absence of signals). MALDI-HRMS spectra of compounds were recorded on a Q-TOF mass spectrometer using 2,5-dihydroxybenzoic acid (DHB) as a matrix and poly(ethylene glycol) (PEG 600) as an internal calibration standard.

**General Protocol for Coupling between 1 and Phenols (ArOH) To Prepare 2W/2X (Description for ∼1.33 mmol Scale).** The appropriate phenol and 2,2′-anhydrouridine **1**[17] were placed in a sealed pressure tube (specific quantities of substrates and reagents given below) and heated (165 °C for **2W**; 175 °C for **2X**) until analytical TLC indicated full conversion (∼2 h). The resulting crude was purified by silica gel column chromatography (2−4% MeOH in $CH_2Cl_2$, v/v) to afford nucleoside **2W**/**2X** (yields specified below).

**2′-*O*-(Napth-2-yl)uridine (2W).** A mixture of 2,2′-anhydrouridine **1** (1.00 g, 4.42 mmol) and 2-napthol (2.40 g, 22.1 mmol) was reacted and purified as described above to afford nucleoside **2W** (0.41 g, 25%) as a light brown solid. $R_f$ 0.4 (10% MeOH in $CH_2Cl_2$, v/v); MALDI-HRMS *m*/*z* 393.1039 ($[M + Na]^+$, $C_{19}H_{18}N_2O_6 \cdot Na^+$, calcd 393.1057); $^1$H NMR (DMSO-$d_6$) δ 11.34 (s, 1H, ex, NH), 8.03 (1H, d, *J* = 8.1 Hz, H6), 7.82−7.85 (ap d, 2H, Nap), 7.73−7.75 (1H, d, *J* = 8.3 Hz, Nap), 7.44−7.48 (ap t, 1H, Nap), 7.41 (d, 1H, *J* = 2.5 Hz, Nap), 7.34−7.37 (ap t, 1H, Nap), 7.23−7.25 (dd, 1H, *J* = 9.1 Hz, *J* = 2.5 Hz, Nap), 6.14 (d, 1H, *J* = 4.9 Hz, H1′), 5.68 (d, 1H, *J* = 8.1 Hz, H5), 5.46 (d, 1H, ex, *J* = 6.4 Hz, 3′-OH), 5.25 (t, 1H, ex, *J* = 5.2 Hz, 5′-OH), 5.02 (ap t, 1H, H2′), 4.43−4.46 (m, 1H, H3′), 4.02−4.05 (m, 1H, H4′), 3.74−3.78 (m, 1H, H5′), 3.65−3.69 (m, 1H, H5′); $^{13}$C NMR (DMSO-$d_6$) δ 162.9, 155.4, 150.5, 140.4 (C6), 133.9, 129.2 (Nap), 128.7, 127.4 (Nap), 126.6 (Nap), 126.4 (Nap), 123.8 (Nap), 118.9 (Nap), 108.9 (Nap), 102.0 (C5), 86.4 (C1′), 85.2 (C4′), 79.3 (C2′), 68.2 (C3′), 60.4 (C5′). Although **2W** is obtained in lower yield than via a recently published microwave-assisted approach (∼50% yield), the current approach does not require access to microwave reactors. The $^1$H NMR data for **2W** are in agreement with the literature report.[18]

**2′-*O*-(Pyren-1-yl)uridine (2X).** A mixture of 2,2′-anhydrouridine **1** (0.30 g, 1.33 mmol) and 1-pyrenol[19] (0.86 g, 3.97 mmol) was reacted and purified as described above to afford nucleoside **2X** (0.26 g, 44%) as a pale yellow solid. $R_f$ 0.4 (10% MeOH in $CH_2Cl_2$, v/v); MALDI-HRMS *m*/*z* 467.1217 ($[M + Na]^+$, $C_{25}H_{20}N_2O_6 \cdot Na^+$, calcd 467.1214); $^1$H NMR (DMSO-$d_6$) δ 11.36 (s, 1H, ex, NH), 8.45 (d, 1H, *J* = 9.3 Hz, Py), 8.20−8.24 (m, 3H, Py), 8.14 (d, 1H, *J* = 9.3 Hz, Py), 7.99−8.09 (m, 4H, H6, Py), 7.86 (1H, d, *J* = 8.5 Hz, Py), 6.35 (d, 1H, *J* = 4.6 Hz, H1′), 5.68 (d, 1H, *J* = 8.2 Hz, H5), 5.63 (br s, 1H, ex, 3′-OH), 5.30 (br s, 1H, ex, 5′-OH), 5.22−5.25 (ap t, 1H, H2′), 4.55−4.56 (m, 1H, H3′), 4.19−4.21 (m, 1H, H4′), 3.81−3.84 (ap d, 1H, H5′), 3.72−3.75 (ap d, 1H, H5′); $^{13}$C NMR (DMSO-$d_6$) δ 162.9, 151.7, 150.5, 140.3 (C6), 131.0, 130.9, 127.1 (Py), 126.4 (Py), 125.6 (Py), 125.2, 125.0 (Py), 124.8 (Py), 124.5 (Py), 124.3 (Py), 123.9, 121.1 (Py), 120.1, 111.9 (Py), 102.0 (C5), 86.6 (C1′), 85.4 (C4′), 80.9 (C2′), 68.5 (C3′), 60.4 (C5′).

**General Protocol for Coupling between 1 and Arylmethyl Alcohol ($ArCH_2OH$) for Preparation of 2Y/2Z (Description for ∼44.2 mmol Scale).** The appropriate aromatic alcohol ($ArCH_2OH$), $NaHCO_3$, and 1.0 M $BH_3$ in THF were placed in a pressure tube, suspended in anhydrous DMSO, and stirred under an argon atmosphere at rt until effervescence ceased (∼10 min). At this point, 2,2′-anhydrouridine **1**[20] was added (specific quantities of substrates and reagents given below), the pressure tube was purged with argon and sealed, and the reaction was heated at ∼160 °C until analytical TLC indicated full conversion (∼3 h). At this point, the reaction mixture was poured into water (200 mL), stirred for 30 min, and diluted with EtOAc (500 mL). The organic phase was washed with water (4 × 200 mL) and evaporated to dryness, and the resulting crude was purified by silica gel column chromatography (2−4%, MeOH in $CH_2Cl_2$, v/v) to afford a residue, which was precipitated from cold acetone to obtain nucleoside **2** (yields specified below).

**2′-*O*-(Pyren-1-yl-methyl)uridine (2Y).** 2,2′-Anhydrouridine **1** (10.00 g, 44.2 mmol), pyren-1-ylmethanol[23] (20.5 g, 88.4 mmol), $NaHCO_3$ (0.73 g. 8.80 mmol), and 1.0 M $BH_3$ in THF (24.5 mL, 22.0 mmol) and anhydrous DMSO (40 mL) were mixed, reacted, worked up, and purified as described above to afford nucleoside **2Y** (5.04 g, 25%) as a white solid. $R_f$ 0.4 (10% MeOH in $CH_2Cl_2$, v/v); MALDI-HRMS *m*/*z* 458.1480 ($[M]^+$, $C_{26}H_{22}N_2O_6^+$, calcd 458.1472); $^1$H NMR (DMSO-$d_6$) δ 11.29 (s, 1H, ex, NH), 8.37−8.39 (d, 1H, *J* = 9.3 Hz, Py), 8.29−8.31 (m, 2H, Py), 8.24−8.26 (d, 1H, *J* = 7.7 Hz, Py), 8.17−8.19 (m, 3H, Py), 8.06−8.12 (m, 2H, Py), 7.82 (d, 1H, *J* = 8.4 Hz, H6), 6.04 (d, 1H, *J* = 5.1 Hz, H1′), 5.43−5.50 (m, 2H, H5, $CH_2$Py), 5.37 (d, 1H, ex, *J* = 5.7 Hz, 3′-OH), 5.28−5.30 (d, 1H, *J* = 12.0 Hz, $CH_2$Py), 5.11 (t, 1H, ex, *J* = 4.9 Hz, 5′-OH), 4.26−4.31 (m, 1H, H3′), 4.18−4.21 (m, 1H, H2′), 3.96−3.97 (m, 1H, H4′), 3.64−3.68 (m, 1H, H5′), 3.59−3.62 (m, 1H, H5′); $^{13}$C NMR (DMSO-$d_6$) δ 162.9, 150.6, 140.1 (C6), 131.4, 130.7, 130.2, 128.7, 127.4 (Py), 127.3 (Py), 127.0 (Py), 126.2 (Py), 125.3 (Py), 124.5 (Py), 124.0 (Py), 123.8, 123.5 (Py), 101.7 (C5), 86.2 (C1′), 85.4 (C4′), 80.9 (C2′), 69.8 ($CH_2$Py), 68.5 (C3′), 60.6 (C5′). $^1$H NMR data for nucleoside **2Y** are in agreement with data where nucleoside **2Y** was obtained via a different route.[17] Full experimental details on the preparation and characterization of **2Y** have, to our knowledge, not been previously published.

**2′-*O*-(Coronen-1-yl-methyl)uridine (2Z).** 2,2′-Anhydrouridine **1** (1.40 g, 6.19 mmol), coronen-1-ylmethanol[24] (4.08 g, 12.4 mmol), $NaHCO_3$ (0.104 g. 1.24 mmol), and 1.0 M $BH_3$ in THF (3.5 mL, 3.1 mmol) and anhydrous DMSO (40 mL) were mixed, reacted, worked

up, and purified as described above with a minor modification. The precipitate that formed upon pouring the reaction mixture into water was collected by filtration, washed with water (3 × 100 mL), and purified by column chromatography to afford nucleoside **2Z** (450 mg, 13%) as a pale yellow solid. $R_f$ 0.4 (10% MeOH in $CH_2Cl_2$, v/v); MALDI-HRMS *m/z* 579.1537 ([M + Na]$^+$, $C_{34}H_{24}N_2O_6 \cdot Na^+$, calcd 579.1532); $^1$H NMR (DMSO-$d_6$) $\delta$ 11.30 (br d, ex, 1H, $J$ = 1.9 Hz, NH), 9.13−9.15 (d, 1H, $J$ = 8.7 Hz, Cor), 8.93−9.03 (m, 10H, Cor), 7.82 (d, 1H, $J$ = 8.0 Hz, H6), 6.18 (d, 1H, $J$ = 4.9 Hz, H1′), 5.85−5.88 (d, 1H, $J$ = 12.1 Hz, $CH_2$Cor), 5.67−5.69 (d, 1H, $J$ = 12.1 Hz, $CH_2$Cor), 5.52 (d, 1H, ex, $J$ = 5.5 Hz, 3′-OH), 5.38 (dd, 1H, $J$ = 8.0 Hz, 1.9 Hz, H5), 5.11 (ap t, 1H, ex, 5′-OH), 4.37−4.43 (m, 2H, H2′, H3′), 4.03−4.06 (m, 1H, H4′), 3.63−3.71 (m, 2H, H5′); $^{13}$C NMR (DMSO-$d_6$) $\delta$ 162.9, 150.6, 140.1 (C6), 132.1, 128.2, 128.1, 127.9, 127.4, 126.5, 126.23 (Cor), 126.20 (Cor), 126.1 (Cor), 126.0 (Cor), 122.5 (Cor), 121.8, 121.5, 121.4, 121.23, 121.17, 101.7 (C5), 86.3 (C1′), 85.5 (C4′), 81.1 (C2′), 70.7 ($CH_2$Cor), 68.6 (C3′), 60.6 (C5′).

**General DMTr-Protection Protocol for the Preparation of 3W−3Z (Description for ∼2.2 mmol Scale).** The appropriate nucleoside **3** (specific quantities given below) was coevaporated twice with anhydrous pyridine (15 mL) and redissolved in anhydrous pyridine. To this were added 4,4′-dimethoxytritylchloride (DMTrCl) and *N*,*N*-dimethyl-4-aminopyridine (DMAP), and the reaction mixture was stirred at rt until TLC indicated complete conversion (∼14 h). The reaction mixture was diluted with $CH_2Cl_2$ (70 mL), and the organic phase was sequentially washed with water (2 × 70 mL) and satd aq $NaHCO_3$ (2 × 100 mL). The organic phase was evaporated to near dryness, and the resulting crude coevaporated with absolute EtOH and toluene (2:1, v/v, 3 × 6 mL) and purified by silica gel column chromatography (0−5%, MeOH in $CH_2Cl_2$, v/v) to afford nucleoside **3** (yields specified below).

**2′-*O*-(Napth-2-yl)-5′-*O*-(4,4′-dimethoxytrityl)uridine (3W).** Nucleoside **2W** (150 mg, 0.40 mmol), DMTrCl (240 mg, 0.60 mmol), and DMAP (∼6 mg) in anhydrous pyridine (7 mL) were mixed, reacted, worked up, and purified as described above to afford nucleoside **3W** (120 mg, 47%) as a pale yellow foam. $R_f$ 0.6 (5%, MeOH in $CH_2Cl_2$, v/v); MALDI-HRMS *m/z* 695.2379 ([M + Na]$^+$, $C_{40}H_{36}N_2O_8 \cdot Na^+$, calcd 695.2364); $^1$H NMR (DMSO-$d_6$) $\delta$ 11.40 (d, 1H, ex, $J$ = 2.1 Hz, NH), 7.83−7.86 (m, 3H, H6, Nap), 7.68 (d, 1H, $J$ = 8.2 Hz, Nap), 7.24−7.45 (m, 13H, DMTr, Nap), 6.90−6.92 (d, 4H, $J$ = 7.1 Hz, DMTr), 6.06 (d, 1H, $J$ = 3.2 Hz, H1′), 5.51 (d, 1H, ex, $J$ = 7.1 Hz, 3′-OH), 5.38−5.40 (m, 1H, H5), 5.12−5.14 (m, 1H, H2′), 4.51−4.55 (m, 1H, H3′), 4.14−4.17 (m, 1H, H4′), 3.75 (s, 6H, 2 × $CH_3$O), 3.32−3.41 (m, 2H, H5′); $^{13}$C NMR (DMSO-$d_6$) $\delta$ 162.9, 158.1, 155.5, 150.3, 144.6, 140.6 (C6), 135.4, 135.2, 133.9, 129.8 (Ar), 129.1 (Nap), 128.8, 127.9 (Ar), 127.7 (Ar), 127.5 (Nap), 126.8 (Ar), 126.6 (Nap), 126.4 (Ar), 123.8 (Ar), 119.0 (Ar), 113.2 (Ar), 109.0 (Ar), 101.8 (C5), 87.6 (C1′), 85.9, 82.6 (C4′), 79.1 (C2′), 68.5 (C3′), 62.7 (C5′), 55.0 ($CH_3$O). The described protocol is similar to an independently developed and recently published protocol; $^{13}$C NMR data recorded in $CDCl_3$ are in agreement with this report.[43] NMR spectra recorded in DMSO-$d_6$ have, to our knowledge, not been provided for this compound.

**2′-*O*-(Pyren-1-yl)-5′-*O*-(4,4′-dimethoxytrityl)uridine (3X).** Nucleoside **2X** (230 mg, 0.52 mmol), DMTrCl (0.30 g, 0.78 mmol), and DMAP (∼9 mg) in anhydrous pyridine (8 mL) were mixed, reacted, worked up, and purified as described above to afford nucleoside **3X** (0.30 g, 78%) as a light yellow foam. $R_f$ 0.6 (5%, MeOH in $CH_2Cl_2$, v/v); MALDI-HRMS *m/z* 769.2504 ([M + Na]$^+$, $C_{46}H_{38}N_2O_8 \cdot Na^+$, calcd 769.2520); $^1$H NMR (DMSO-$d_6$) $\delta$ 11.32 (s, 1H, ex, NH), 8.49 (d, 1H, $J$ = 9.2 Hz, Py), 8.20−8.24 (m, 3H, Py), 8.14 (d, 1H, $J$ = 9.2 Hz, Py), 8.08−8.10 (d, 1H, $J$ = 9.1 Hz, Py), 7.99−8.04 (m, 2H, Py), 7.86−7.89 (m, 2H, H6, Py), 7.43−7.45 (m, 2H, DMTr), 7.24−7.36 (m, 7H, DMTr), 6.90−6.92 (m, 4H, DMTr), 6.25 (d, 1H, $J$ = 3.2 Hz, H1′), 5.69 (d, 1H, ex, $J$ = 6.8 Hz, 3′-OH), 5.38 (d, 1H, $J$ = 8.2 Hz, H5), 5.35−5.37 (m, 1H, H2′), 4.61−4.65 (m, 1H, H3′), 4.34−4.37 (m, 1H, H4′), 3.74 (s, 6H, 2 × $CH_3$O), 3.46−3.50 (m, 1H, H5′), 3.38−3.41 (m, 1H, H5′); $^{13}$C NMR (DMSO-$d_6$) $\delta$ 162.9, 158.1, 151.7, 150.3, 144.6, 140.5 (C6), 135.4, 135.1, 131.1, 131.0, 129.78 (DMTr), 129.76 (DMTr), 127.9 (DMTr), 127.1 (Py), 126.8 (DMTr), 126.4 (Py), 125.6 (Py), 125.3, 125.1 (Py), 124.9, 124.5 (Py), 124.3 (Py), 124.0, 121.2 (Py), 120.1, 113.2 (DMTr), 112.3 (Py), 101.7 (C5), 87.8 (C1′), 85.9, 82.7 (C4′), 80.7 (C2′), 68.7 (C3′), 62.7 (C5′), 55.0 ($CH_3$O).

**2′-*O*-(Pyren-1-yl-methyl)-5′-*O*-(4,4′-dimethoxytrityl)uridine (3Y).** Nucleoside **2Y** (1.02 g, 2.20 mmol), DMTrCl (1.29 g, 3.30 mmol), and DMAP (∼18 mg) in anhydrous pyridine (20 mL) were mixed, reacted, worked up, and purified as described above to afford **3Y** (1.20 g, 72%) as pale yellow foam. $R_f$ 0.6 (5%, MeOH in $CH_2Cl_2$, v/v); MALDI-HRMS *m/z* 783.2698 ([M + Na]$^+$, $C_{47}H_{40}N_2O_8 \cdot Na^+$, calcd 783.2677); $^1$H NMR (DMSO-$d_6$) $\delta$ 11.36 (d, 1H, ex, $J$ = 1.9 Hz, NH), 8.41−8.43 (d, 1H, $J$ = 9.3 Hz, Py), 8.30−8.32 (m, 2H, Py), 8.14−8.25 (m, 5H, Py), 8.07−8.10 (t, 1H, $J$ = 7.7 Hz, Py), 7.63 (d, 1H, $J$ = 8.1 Hz, H6), 7.17−7.34 (m, 9H, DMTr), 6.82−6.86 (m, 4H, DMTr), 6.02 (d, 1H, $J$ = 3.9 Hz, H1′), 5.48−5.50 (d, 1H, $J$ = 12.1 Hz, $CH_2$Py), 5.45 (d, 1H, ex, $J$ = 6.3 Hz, 3′-OH), 5.36−5.38 (d, 1H, $J$ = 12.1 Hz, $CH_2$Py), 5.13 (dd, 1H, $J$ = 8.1 Hz, 1.9 Hz, H5), 4.34−4.38 (m, 1H, H3′), 4.21−4.24 (m, 1H, H2′), 4.05−4.09 (m, 1H, H4′), 3.71 (s, 3H, $CH_3$O), 3.69 (s, 3H, $CH_3$O), 3.20−3.24 (m, 2H, H5′); $^{13}$C NMR (DMSO-$d_6$) $\delta$ 162.8, 158.08, 158.06, 150.4, 144.5, 140.0 (C6), 135.3, 135.0, 131.3, 130.7, 130.2, 129.71 (DMTr), 129.66 (DMTr), 128.7, 127.8 (DMTr), 127.6 (DMTr), 127.4 (Py), 127.3 (Py), 127.0 (Py), 126.7 (DMTr), 126.2 (Py), 125.3 (Py), 124.5 (Py), 124.0, 123.8, 123.4 (Py), 113.20 (DMTr), 113.17 (DMTr), 101.4 (C5), 87.1 (C1′), 85.9, 83.1 (C4′), 80.6 (C2′), 69.9 ($CH_2$Py), 68.7 (C3′), 62.8 (C5′), 55.0 ($CH_3$O). The protocol and $^1$H NMR data recorded in $CDCl_3$ for **3Y** are in agreement with those from a related protocol.[17] Full experimental details on the preparation and characterization of **3Y** have not been previously reported.

**2′-*O*-(Coronen-1-yl-methyl)-5′-*O*-(4,4′-dimethoxytrityl)-uridine (3Z).** Nucleoside **2Z** (250 mg, 0.45 mmol), DMTrCl (262 mg, 0.67 mmol), and DMAP (∼15 mg) in anhydrous pyridine (6 mL) were mixed, reacted, worked up, and purified as described above to afford nucleoside **3Z** (245 mg 63%) as a yellow foam. $R_f$ 0.6 (5%, MeOH in $CH_2Cl_2$, v/v); MALDI-HRMS *m/z* 881.2824 ([M + Na]$^+$, $C_{55}H_{42}N_2O_8 \cdot Na^+$, calcd 881.2839); $^1$H NMR (DMSO-$d_6$) $\delta$ 11.40 (br d, 1H, ex, $J$ = 1.9 Hz, NH), 9.14−9.16 (d, 1H, $J$ = 8.8 Hz, Cor), 8.96−9.02 (m, 9H, Cor), 8.88−8.90 (d, 1H, $J$ = 8.5 Hz, Cor), 7.63 (d, 1H, $J$ = 8.1 Hz, H6), 7.29−7.31 (d, 2H, $J$ = 7.4 Hz, DMTr), 7.11−7.22 (m, 7H, DMTr), 6.74−6.79 (m, 4H, DMTr), 6.18 (d, 1H, $J$ = 4.1 Hz, H1′), 5.87−5.90 (d, 1H, $J$ = 12.6 Hz, $CH_2$Cor), 5.75−5.78 (d, 1H, $J$ = 12.6 Hz, $CH_2$Cor), 5.59 (d, 1H, ex, $J$ = 6.3 Hz, 3′-OH), 5.06 (dd, 1H, $J$ = 8.1 Hz, 1.9 Hz, H5), 4.46−4.50 (m, 1H, H3′), 4.40−4.43 (m, 1H, H2′), 4.15−4.18 (m, 1H, H4′), 3.63 (s, 3H, $CH_3$O), 3.58 (s, 3H, $CH_3$O), 3.32−3.34 (m, 1H, H5′), 3.25−3.27 (m, 1H, H5′); $^{13}$C NMR (DMSO-$d_6$) $\delta$ 162.8, 158.02, 157.97, 150.4, 144.4, 140.0 (C6), 135.3, 135.0, 132.2, 129.7 (DMTr), 129.6 (DMTr), 128.3, 128.2, 128.0, 127.7 (DMTr), 127.59 (DMTr), 127.56, 126.61 (DMTr), 126.59, 126.41 (Cor), 126.36 (Cor), 126.3 (Cor), 126.23 (Cor), 126.21, 126.19, 126.1 (Cor), 122.6 (Cor), 121.9, 121.6, 121.5, 121.4, 121.35, 121.28, 113.13 (DMTr), 113.09 (DMTr), 101.4 (C5), 87.1 (C1′), 85.9, 83.2 (C4′), 80.7 (C2′), 70.7 ($CH_2$Cor), 68.8 (C3′), 62.8 (C5′), 54.9 ($CH_3$O), 54.8 ($CH_3$O).

**General Phosphitylation Protocol for the Preparation of 4W−4Z (Description for ∼1 mmol Scale).** The appropriate nucleoside **3** (specific quantities of substrates and reagents given below) was coevaporated with anhydrous 1,2-dicholoroethane (4 mL) and redissolved in anhydrous $CH_2Cl_2$. To this were added *N*,*N*-diisopropylethylamine (DIPEA) and 2-cyanoethyl-*N*,*N*-diisopropylchlorophosporamidite (PCl reagent), and the reaction mixture was stirred at rt until TLC indicated complete conversion (∼3 h), whereupon absolute EtOH (2 mL) and $CH_2Cl_2$ (20 mL) were sequentially added to the

solution. The organic phase was washed with satd aq $NaHCO_3$ (10 mL) and evaporated to near dryness, and the resulting residue was purified by silica gel column chromatography (40−70% EtOAc in petroleum ether, v/v) to afford the corresponding phosphoramidite **4** (yields specified below).

**2′-*O*-(Napth-2-yl)-3′-*O*-(*N*,*N*-diisopropylamino-2-cyanoethoxyphosphinyl)-5′-*O*-(4,4′-dimethoxytrityl)uridine (4W).** Nucleoside **3W** (100 mg, 0.15 mmol), DIPEA (106 μL, 0.59 mmol), and PCl reagent (66 μL, 0.23 mmol) in anhydrous $CH_2Cl_2$ (1.5 mL) were mixed, reacted, worked up, and purified as described above to afford phosphoramidite **4W** (95 mg, 74%) as a white foam. $R_f$ 0.8 (5% MeOH in $CH_2Cl_2$, v/v); MALDI-HRMS *m/z* 895.3462 ($[M + Na]^+$, $C_{49}H_{53}N_4O_9P \cdot Na^+$, calcd 895.3448); $^{31}P$ NMR ($CDCl_3$) δ 151.0, 150.9. The reaction yield compares favorably with an independently developed protocol utilizing 2-cyanoethyl *N*,*N*,*N*′,*N*′-tetraisopropylphosphorodiamidite ($PN_2$ reagent) and 1*H*-tetrazole as phosphitylation reagent and activator, respectively (∼61% yield).[40] The $^{31}P$ NMR data are in agreement with literature data.[43]

**3′-*O*-(*N*,*N*-Diisopropylamino-2-cyanoethoxyphosphinyl)-2′-*O*-(pyren-1-yl)-5′-*O*-(4,4′-dimethoxytrityl)uridine (4X).** Nucleoside **3X** (0.28 g, 0.38 mmol), DIPEA (268 μL, 1.50 mmol), and PCl reagent (167 μL, 0.75 mmol) in anhydrous $CH_2Cl_2$ (2.5 mL) were mixed, reacted, worked up, and purified as described above to afford phosphoramidite **4X** (0.27 g, 76%) as a white foam. $R_f$ 0.8 (5% MeOH in $CH_2Cl_2$, v/v); MALDI-HRMS *m/z* 969.3608 ($[M + Na]^+$, $C_{55}H_{55}N_4O_9P \cdot Na^+$, calcd 969.3604); $^{31}P$ NMR ($CDCl_3$) δ 149.8, 149.4.

**3′-*O*-(*N*,*N*-Diisopropylamino-2-cyanoethoxyphosphinyl)-2′-*O*-(pyren-1-yl-methyl)-5′-*O*-(4,4′-dimethoxytrityl)uridine (4Y).** Nucleoside **3Y** (0.58 g, 0.76 mmol), DIPEA (0.53 mL, 3.05 mmol), and PCl reagent (340 μL, 1.53 mmol) in anhydrous $CH_2Cl_2$ (5 mL) were mixed, reacted, worked up, and purified as described above to afford phosphoramidite **4Y** (0.56 g, 76%) as a white foam. $R_f$ 0.8 (5% MeOH in $CH_2Cl_2$, v/v); MALDI-HRMS *m/z* 983.3767 ($[M + Na]^+$, $C_{56}H_{57}N_4O_9P \cdot Na^+$, calcd 983.3761); $^{31}P$ NMR ($CDCl_3$) δ 150.3, 150.2. The observed reaction yield and $^{31}P$ NMR data are comparable to the reported protocol that utilizes $PN_2$ reagent and 1*H*-tetrazole as phosphitylation reagent and activator, respectively.[14] HRMS data have not been previously reported for this compound.

**2′-*O*-(Coronen-1-yl-methyl)-3′-*O*-(*N*,*N*-diisopropylamino-2-cyanoethoxyphosphinyl)-5′-*O*-(4,4′-dimethoxytrityl)-uridine (4Z).** Nucleoside **3Z** (240 mg, 0.28 mmol), DIPEA (200 μL, 1.11 mmol), and PCl reagent (125 μL, 0.56 mmol) in anhydrous $CH_2Cl_2$ (6 mL) were mixed, reacted, worked up, and purified as described above to afford phosphoramidite **4Z** (230 mg, 78%) as a light yellow foam. $R_f$ 0.8 (5% MeOH in $CH_2Cl_2$, v/v); MALDI-HRMS *m/z* 1081.3864 ($[M + Na]^+$, $C_{64}H_{59}N_4O_9P \cdot Na^+$, calcd 1081.3917); $^{31}P$ NMR ($CDCl_3$) δ 150.2.

**2′-Amino-2′-deoxy-2′-*N*-methyl-2′-*N*-(pyren-1-yl-methyl)-5′-*O*-(4,4′-dimethoxytrityl)uridine (6Q).** Known nucleoside **5**[27] (200 mg, 0.36 mmol) was coevaporated with anhydrous 1, 2-dichloroethane (2 × 4 mL) and redissolved in anhydrous THF (5 mL). Pyrene-1-ylmethylchloride (205 mg, 0.37 mmol) and triethylamine (0.52 mL, 3.73 mmol) were added, and the reaction mixture was heated at reflux for 2 days, whereupon the solvent was evaporated off. The crude residue was taken up in a mixture of $CHCl_3$ and satd aq $NaHCO_3$ (50 mL, 3:2, v/v), and the layers were separated. The aqueous phase was extracted with $CHCl_3$ (2 × 20 mL), and the combined organic phase was evaporated to dryness. The resulting residue was purified by silica gel column chromatography (0−1.25% MeOH/$CH_2Cl_2$, v/v) to afford nucleoside **6Q** as a yellow foam (129 mg, 46%). $R_f$ 0.5 (60%, EtOAc in petroleum ether, v/v); MALDI-HRMS *m/z* 774.3156 ($[M + H]^+$ $C_{48}H_{43}N_3O_7 \cdot H^+$, Calc 774.3174); $^1H$ NMR (DMSO-$d_6$) δ 11.41 (d, 1H, ex, *J* = 1.7 Hz, NH), 8.50 (d, 1H, *J* = 9.1 Hz, Py), 8.01−8.29 (m, 8H, Py), 7.63 (d, 1H, *J* = 8.2 Hz, H6), 7.20−7.38 (m, 9H, DMTr), 6.85−6.89 (m, 4H, DMTr), 6.43 (d, 1H, *J* = 8.2 Hz, H1′), 5.56 (d, 1H, ex, *J* = 5.2 Hz, 3′-OH), 5.43 (dd, 1H, *J* = 8.3 Hz, 1.7 Hz, H5), 4.41−4.50 (m, 3H, $CH_2$Py, H3′), 4.06−4.08 (m, 1H, H4′), 3.71 (s, 3H, $CH_3O$), 3.70 (s, 3H, $CH_3O$), 3.44−3.48 (dd, 1H, *J* = 8.3 Hz, 8.1 Hz, H2′), 3.28−3.31 (m, 1H, H5′, overlap with $H_2O$), 3.16−3.20 (dd, 1H, *J* = 10.6 Hz, 3.6 Hz, H5′), 2.33 (s, 3H, $CH_3N$); $^{13}C$ NMR (DMSO-$d_6$) δ 162.7, 158.08, 158.07, 150.6, 144.5, 140.2 (C6), 135.4, 135.1, 132.7, 130.7, 130.3, 130.2, 129.71 (DMTr), 129.67 (DMTr), 129.2, 128.0 (Py), 127.8 (DMTr), 127.6 (DMTr), 127.3 (Py), 126.9 (Py), 126.8 (Py), 126.7 (DMTr), 126.1 (Py), 125.01, 124.98 (Py), 124.4 (Py), 124.1, 124.0 (Py), 123.9, 113.20 (DMTr), 113.17 (DMTr), 102.1 (C5), 85.9, 85.1 (C4′), 83.4 (C1′), 71.3 (C3′), 67.8 (C2′), 64.1 (C5′), 57.4 ($CH_2$Py), 55.0 ($CH_3O$), 38.6 ($CH_3N$). $^{13}C$ NMR data recorded in $CDCl_3$ are in agreement with literature reports where **6Q** was obtained via a different synthetic route.[15] Full experimental details on the preparation and characterization of **6Q** have not been previously published.

**2′-Amino-2′-deoxy-2′-*N*-methyl-2′-*N*-(pyren-1-yl-carbonyl)-5′-*O*-(4,4′-dimethoxytrityl)uridine (6S).** Nucleoside **5**[27] (150 mg, 0.27 mmol) was coevaporated with anhydrous 1,2-dichloroethane (2 × 5 mL), dissolved in anhydrous DMF (4.5 mL), and added to a prestirred (1 h at rt) solution of 1-pyrenecarboxylic acid (100 mg, 0.40 mmol), *O*-(7-azabenzotriazole-1-yl)-*N*,*N*,*N*′,*N*′-tetramethyluronium hexafluorophosphate (HATU, 125 mg, 0.32 mmol) and DIPEA (0.12 mL, 0.70 mmol) in anhydrous DMF (4.5 mL). The reaction mixture was stirred for 17 h, whereupon it was diluted with EtOAc (50 mL) and sequentially washed with satd aq $NaHCO_3$ (20 mL) and $H_2O$ (2 × 20 mL). The organic phase was evaporated to dryness, and the resulting residue was purified by silica gel column chromatography (0−2% MeOH in $CH_2Cl_2$, v/v) to afford nucleoside **6S** as a white foam (164 mg, 78%). $R_f$ 0.4 (5% MeOH in $CH_2Cl_2$, v/v). MALDI-HRMS *m/z* 788.2985 ($[M + H]^+$, $C_{48}H_{41}N_3O_8 \cdot H^+$, calcd 788.2966); $^1H$ NMR ($CDCl_3$) δ 8.65 (br s, 1H, NH, ex), 7.97−8.28 (m, 9H, Py), 7.85 (d, 1H, *J* = 8.3 Hz, H6), 7.20−7.44 (m, 9H, DMTr), 6.80−6.90 (m, 4H, DMTr), 6.78 (d, 1H, *J* = 6.0 Hz, H1′), 5.42−5.48 (m, 1H, H5), 4.80−4.90 (m, 2H, H2′, H3′), 4.28−4.43 (m, 1H, H4′), 3.77 (s, 6H, $CH_3O$), 3.48−3.63 (m, 2H, H5′), 2.98 (s, 3H, $NCH_3$), traces of a second rotamer are observed; $^{13}C$ NMR ($CDCl_3$) δ 174.4, 162.9, 159.0, 150.5, 144.5, 140.0 (C6), 135.6, 135.5, 132.3, 131.4, 131.0, 130.44 (DMTr), 130.42 (DMTr), 129.4 (Py), 128.7 (Py), 128.5 (DMTr), 128.3 (DMTr), 127.4, 126.7 (Py), 126.1 (Py), 126.0 (Py), 125.0 (Py), 124.8, 124.7, 124.3 (Py), 113.6 (DMTr), 113.3 (DMTr), 103.2 (C5), 87.3, 86.6 (C4′), 85.3 (C1′), 71.8 (C3′/C2′), 65.8 (C2′/C3′), 63.0 (C5′), 55.5 ($CH_3O$), 38.5 ($NCH_3$). A trace impurity of grease was observed at 29.9 ppm.

**2′-Amino-2′-deoxy-2′-*N*-methyl-2′-*N*-(pyren-1-yl-methyl-carbonyl)-5′-*O*-(4,4′-dimethoxytrityl)uridine (6V).** Known nucleoside **5**[27] (158 mg, 0.28 mmol) was coevaporated with 1,2-dichloroethane (2 × 5 mL) and subsequently dissolved in anhydrous $CH_2Cl_2$ (8 mL). To this was added 1-ethyl-3-(3-dimethylamino-propyl) carbodiimide hydrochloride (EDC·HCl, 73 mg, 0.38 mmol) and pyrene-1-ylacetic acid (108 mg, 0.41 mmol). The reaction mixture was stirred under argon at rt for 3 h whereupon the reaction mixture was diluted with $CH_2Cl_2$ (30 mL) and sequentially washed with satd aq $NaHCO_3$ (20 mL) and $H_2O$ (3 × 15 mL). The organic phase was evaporated to dryness and the resulting residue was purified by silica gel column chromatography (0−3% *i*-PrOH/$CH_2Cl_2$, v/v) to afford a rotameric mixture (2:5 by $^1$HNMR) of nucleoside **6V** (187 mg, 83%) as a brown foam. $R_f$ 0.5 (5%, *i*-PrOH in $CH_2Cl_2$, v/v); MALDI-HRMS *m/z* 801.3078 ($[M]^+$, $C_{49}H_{43}N_3O_8$, calcd 801.3045); $^1H$ NMR (DMSO-$d_6$) δ 11.52 (d, 1H, *J* = 1.7 Hz, $NH_{(A)}$), 11.46 (d, 0.4H, *J* = 1.7 Hz, $NH_{(B)}$), 8.05−8.31 (m, 11.2H, $Py_{(A)}$ + $Py_{(B)}$), 7.89 (d, 1H, *J* = 7.8 Hz, $Py_{(A)}$), 7.82 (d, 0.4H, *J* = 7.8 Hz, $Py_{(B)}$), 7.67−7.70 (m, 1.4H, $H6_{(A)}$ + $H6_{(B)}$), 7.13−7.43 (m, 12.6H, $DMT_{(A+B)}$), 6.78−6.87 (m, 5.6H, $DMT_{(A+B)}$), 6.42 (d, 1H, *J* = 8.0 Hz, $H1'_{(A)}$), 6.31 (d, 0.4H, *J* = 5.5 Hz, $H1'_{(B)}$), 5.92 (d, 0.4H, ex, *J* = 4.9 Hz, $3'\text{-}OH_{(B)}$), 5.76 (d, 1H, ex, *J* = 4.9 Hz, 3′-

$OH_{(A)}$), 5.38 (dd, 1H, $J$ = 8.2 Hz, 1.7 Hz, $H5_{(A)}$), 5.33 (dd, 0.4H, $J$ = 8.2 Hz, 1.7 Hz, $H5_{(B)}$), 5.11−5.17 (m, 1H, $H2'_{(A)}$), 4.80−4.86 (m, 0.4H, $H2'_{(B)}$), 4.58−4.63 (d, 1H, $J$ = 16.5 Hz, $CH_2Py_{(A)}$), 4.51−4.56 (d, 0.4H, $J$ = 16.5 Hz, $CH_2Py_{(B)}$), 4.37−4.49 (m, 2.4H, 1 x $CH_2Py_{(A)}$, $H3'_{(A)}$, $H3'_{(B)}$), 4.30−4.37 (d, 0.4H, $J$ = 16.5 Hz, $CH_2Py_{(B)}$), 4.10−4.16 (m, 1.4H, $H4'_{(A)}$ + $H4'_{(B)}$), 3.68 (s, 2.4H, $CH_3O_{(B)}$), 3.64 (s, 3H, $CH_3O_{(A)}$), 3.62 (s, 3H, $CH_3O_{(A)}$), 3.35−3.37 (m, 0.4H, $H5'_{(B)}$), 3.32 (s, 3H, $CH_3N_{(A)}$), 3.29−3.32 (m, 1H, $H5'_{(A)}$, overlap with $H_2O$), 3.23−3.27 (dd, 0.4H, $J$ = 10.6 Hz, 2.6 Hz, $H5'_{(B)}$), 3.15−3.19 (dd, 1H, $J$ = 10.6 Hz, 2.6 Hz, $H5'_{(A)}$), 3.03 (s, 1.2H, $CH_3N_{(B)}$); $^{13}$C NMR (DMSO-$d_6$) $\delta$ 172.2, 172.1, 162.81, 162.78, 158.06, 158.03, 158.02, 150.5, 150.4, 144.6, 144.3, 140.2 ($C6_{(B)}$), 140.1 ($C6_{(A)}$), 135.4, 135.3, 135.2, 135.0, 130.7, 130.62, 130.56, 130.3, 130.2, 129.71 (DMTr), 129.69 (DMTr), 129.1, 128.1 (Py-$CH_A$), 127.9 (Py-$CH_B$), 127.8 (DMTr), 127.73 (DMTr), 127.70 (DMTr), 127.3 (Py), 127.14 (Py), 127.10 (Py), 126.73 (Py), 126.66 (DMTr), 126.1 (Py), 125.1 (Py), 125.0 (Py), 124.9 (Py), 124.5 (Py), 124.1, 124.0, 123.85 (Py), 123.76 (Py), 113.2 (DMTr), 113.1 (DMTr), 102.2 ($C5_{(A)}$), 102.0 ($C5_{(B)}$), 85.9, 85.7, 85.5 ($C1'_{(B)}$), 85.2 ($C4'_{(A)}$), 84.8 ($C4'_{(B)}$), 83.2 ($C1'_{(A)}$), 70.5 ($C3'_{(A)}$), 69.3 ($C3'_{(B)}$), 63.8 ($C5'_{(A)}$), 63.7 ($C5'_{(B)}$), 62.1 ($C2'_{(B)}$), 59.0 ($C2'_{(A)}$), 54.92 ($CH_3O_{(B)}$), 54.87 ($CH_3O_{(B)}$), 54.85 ($CH_3O_{(A)}$), 54.82 ($CH_3O_{(A)}$), 38.1 ($CH_2Py_{(A)}$), 37.8 ($CH_2$-$Py_{(B)}$), 34.2 ($CH_3N_{(A)}$), 31.4 ($CH_3N_{(B)}$).

**2′-Amino-2′-deoxy-2′-*N*-methyl-2′-*N*-(pyren-1-yl-methyl)-3′-*O*-(*N*,*N*-diisopropylamino-2-cyanoethoxyphosphinyl)-5′-*O*-(4,4′-dimethoxytrityl)uridine (7Q).** Nucleoside **6Q** (135 mg, 0.18 mmol) was coevaporated with $CH_3CN$ (2 × 4 mL) and redissolved in anhydrous $CH_3CN$ (2.5 mL). To this were added DIPEA (153 $\mu$L, 0.87 mmol) and PCl reagent (78 $\mu$L, 0.35 mmol). The reaction mixture was stirred at rt for 4 h, whereupon it was cooled on an ice bath and abs EtOH (3 mL) was added. The solvent was evaporated off, and the resulting residue purified by silica gel column chromatography (0−40% EtOAc in petroleum ether, v/v; column built in 0.5% $Et_3N$) to afford nucleoside **6Q** as a white foam (97 mg, 57%). $R_f$ 0.3 (40% EtOAc in petroleum ether, v/v); MALDI-HRMS $m/z$ 996.4046 ([M + Na]$^+$, $C_{57}H_{60}N_5O_8P\cdot Na^+$, calcd 996.4077); $^{31}$P NMR ($CDCl_3$) $\delta$ 151.0, 149.8. The $^{31}$P NMR data are in general agreement with literature data.[15]

**2′-Amino-2′-deoxy-2′-*N*-methyl-3′-*O*-(*N*,*N*-diisopropylamino-2-cyanoethoxyphosphinyl)-2′-*N*-(pyren-1-yl-carbonyl)-5′-*O*-(4,4′-dimethoxytrityl)uridine (7S).** Nucleoside **6S** (219 mg, 0.28 mmol) was coevaporated with anhydrous 1,2-dicholoroethane (2 × 2 mL) and redissolved in anhydrous $CH_2Cl_2$ (2 mL). To this was added DIPEA (58 $\mu$L, 0.33 mmol) followed by dropwise addition of PCl reagent (74 $\mu$L, 0.33 mmol). After 2 h of stirring at rt, $CH_2Cl_2$ (10 mL) was added, and the reaction mixture stirred for additional 10 min, whereupon the solvent was evaporated under reduced pressure. The resulting residue was purified by silica gel column chromatography (1st column: 0−40% EtOAc in petroleum ether, v/v; second column: 0−4% MeOH in $CH_2Cl_2$, v/v) to afford a rotameric mixture of phosphoramidite **7S** as a white foam (138 mg, 49%). $R_f$ 0.8 (5% MeOH in $CH_2Cl_2$, v/v); MALDI-HRMS $m/z$ 1010.3865 ([M + Na]$^+$, $C_{57}H_{58}N_5O_9P\cdot Na^+$, calcd 1010.3870); $^{31}$P NMR ($CDCl_3$) $\delta$ 151.8, 151.2, 150.8.

**2′-Amino-2′-deoxy-2′-*N*-methyl-3′-*O*-(*N*,*N*-diisopropylamino-2-cyanoethoxyphosphinyl)-2′-*N*-(pyren-1-yl-methylcarbonyl)-5′-*O*-(4,4′-dimethoxytrityl)uridine (7V).** Nucleoside **6V** (0.30 g, 0.37 mmol) was coevaporated with anhydrous 1,2-dicholoroethane (2 × 3 mL) and redissolved in anhydrous $CH_2Cl_2$ (4 mL). To this was added DIPEA (0.32 mL, 1.84 mmol) followed by dropwise addition of PCl reagent (0.16 mL, 0.74 mmol). After stirring for 1.5 h at rt, $CH_2Cl_2$ (10 mL) was added, and the reaction mixture was stirred for additional 10 min, whereupon the solvent was evaporated under reduced pressure. The resulting residue was purified by silica gel column chromatography (0−60% EtOAc in petroleum ether, v/v) to afford phosphoramidite **7V** as a bright yellow foam (153 mg, 42%). $R_f$ 0.4 (60% EtOAc in petroleum ether, v/v); MALDI-HRMS $m/z$ 1024.4037 ([M + Na]$^+$, $C_{58}H_{60}N_5O_9P\cdot Na^+$, calcd 1024.4026); $^{31}$P NMR ($CDCl_3$) $\delta$ 150.6, 150.5.

**Synthesis and Purification of ONs.** Synthesis of modified oligodeoxyribonucleotides (ONs) was performed on an DNA synthesizer using 0.2 $\mu$mol scale succinyl linked LCAA-CPG (long chain alkyl amine controlled pore glass) columns with a pore size of 500 Å. Standard protocols for incorporation of DNA phosphoramidites were used. A ∼50-fold molar excess of modified phosphoramidites in anhydrous acetonitrile (at 0.05 M) was used during hand-couplings (performed to conserve material) except with **4Z** (∼70-fold molar excess in anhydrous $CH_2Cl_2$, at 0.07M). Moreover, extended oxidation (45 s) and coupling times were used (0.01 M 4,5-dicyanoimidazole as activator, 15 min for monomers **V**, **W**, and **Y**, 35 min for monomer **Z**; 0.01 M 5-(bis-3,5-trifluoromethylphenyl)-1*H*-tetrazole [Activator 42], 15 min for monomers **Q**, **S**, and **V**). Cleavage from solid support and removal of protecting groups were accomplished upon treatment with 32% aq ammonia (55 °C, 24 h). Purification of all modified ONs was performed to minimum 80% purity using either of two methods: (a) overall synthesis yield >80%: cleavage of DMT using 80% aq. AcOH, followed by precipitation from acetone (−18 °C for 12−16 h) and washing with acetone, or (b) overall synthesis yield <80%: purification of ONs by RP-HPLC as described below, followed by detritylation and precipitation as outlined under "a".

Purification of the crude ONs was performed on a HPLC system equipped with an XTerra MS C18 precolumn (10 $\mu$m, 7.8 × 10 mm) and a XTerra MS C18 column (10 $\mu$m, 7.8 × 150 mm) using the representative gradient protocol depicted in Table S1 in Supporting Information. The identity of synthesized ONs was established through MALDI-MS/MS analysis (Tables S2−S3 in Supporting Information) recorded in positive ions mode on a quadrupole time-of-flight tandem mass spectrometer equipped with a MALDI source using anthranilic acid as a matrix, while purity (>80%) was verified by RP-HPLC running in analytical mode.

**Thermal Denaturation Studies.** Concentrations of ONs were estimated using the following extinction coefficients for DNA (OD/$\mu$mol): G (12.01), A (15.20), T (8.40), C (7.05); for RNA (OD/$\mu$mol): G (13.70), A (15.40), U (10.00), C (9.00); for fluorophores (OD/$\mu$mol): naphthalene (3.75),[18] pyrene (22.4),[10] and coronene (36.0).[44] Each strand was thoroughly mixed and denatured by heating to 70−85 °C followed by cooling to the starting temperature of the experiment. Quartz optical cells with a path length of 1.0 cm were used. Thermal denaturation temperatures ($T_m$ values [°C]) of duplexes (1.0 $\mu$M final concentration of each strand) were measured on a UV−vis spectrophotometer equipped with a 12-cell Peltier temperature controller and determined as the maximum of the first derivative of the thermal denaturation curve ($A_{260}$ vs $T$) recorded in medium salt buffer ($T_m$ buffer: 100 mM NaCl, 0.1 mM EDTA, and pH 7.0 adjusted with 10 mM $Na_2HPO_4$ and 5 mM $Na_2HPO_4$). The temperature of the denaturation experiments ranged from at least 15 °C below $T_m$ to 20 °C above $T_m$ (although not below 1 °C). A temperature ramp of 0.5 °C/min was used in all experiments. Reported $T_m$ values are averages of two experiments within ±1.0 °C.

**Steady-State Fluorescence Emission Spectra.** Steady-state fluorescence emission spectra of ONs modified with pyrene-functionalized monomers **Q**, **S**, **V**, **X**, and **Y** and the corresponding duplexes with cDNA/RNA targets were recorded in nondeoxygenated thermal denaturation buffer (each strand 1.0 $\mu$M) and obtained as an average of five scans using an excitation wavelength of $\lambda_{ex}$ = 350 nm, excitation slit 5.0 nm, emission slit 2.5 nm, and a scan speed of 600 nm/min. Experiments were determined at 5 °C to ascertain maximal hybridization of probes to DNA/RNA targets. Solutions were heated to 80 °C followed by cooling to 5 °C over 10 min.

## ■ ASSOCIATED CONTENT

**Supporting Information.** Additional discussion regarding formation of cyclic N2′,O3′-hemiaminal ether (Scheme S1); representative RP-HPLC protocol (Table S1); MALDI-MS of ONs (Tables S2 and S3); representative thermal denaturation curves (Figures S1 and S2); discussion of RNA mismatch data for **B2** series (Table S4 and Figure S3); absorption data (Figure S4 and Tables S5 and S6); and steady-state fluorescence emission spectra (Figures S5−S9) for modified ONs; additional discussion of fluorescence emission spectra; NMR spectra of compounds **2**−**7**. This material is available free of charge via the Internet at http://pubs.acs.org.

## ■ AUTHOR INFORMATION

### Corresponding Author

*E-mail: hrdlicka@uidaho.edu.

### Author Contributions

§These authors contributed equally to this work.

## ■ ACKNOWLEDGMENT

P.J.H. appreciates support from Award Number R01 GM-088697 from the National Institute of General Medical Sciences, National Institutes of Health; Institute of Translational Health Sciences (ITHS) (supported by grants UL1 RR025014, KL2 RR025015, and TL1 RR025016 from the NIH National Center for Research Resources); NIH Grant Number P20 RR016454 from the INBRE Program of the National Center for Research Resources; Idaho NSF EPSCoR and a Univ. Idaho Research Office and Research Council Seed Grant. S.K. and B.A.A. enjoy support from the Student Grant Program at University of Idaho (U80203 & U80077). P.N. and T.B.J. appreciate support from the The Danish National Research Foundation. We thank Dr. Lee Deobald and Prof. Andrzej J. Paszczynski (EBI Murdock Mass Spectrometry Center) for mass spectrometric analyses. Input from Todd Pankratz, Joanna Hawryluk, and Johanna Root during preliminary phases of this study and scholarships from the National Science Foundation under award number 0648202 and the Department of Defense ASSURE (Awards to Stimulate and Support Undergraduate Research Experiences) Program supporting J.H. and J.R. are appreciated.

## ■ REFERENCES

(1) Bell, N. M.; Micklefield, J. *ChemBioChem* **2009**, *10*, 2691–2703.
(2) Duca, M.; Vekhoff, P.; Halby, L.; Arimondo, P. B. *Nucleic Acids Res.* **2008**, *36*, 5123–5138.
(3) (a) Bennett, F. C.; Swayze, E. E. *Annu. Rev. Pharmacol. Toxicol.* **2010**, *50*, 259–293. (b) Watts, J. K.; Deleavey, G. F.; Damha, M. J. *Drug Discovery Today* **2008**, *13*, 842–855.
(4) (a) Juskowiak, B. *Anal. Bioanal. Chem.* **2011**, *399*, 3157–3176. (b) Dodd, D. W.; Hudson, R. H. E. *Mini-Rev. Org. Chem.* **2009**, *6*, 378–391. (c) Asseline, U. *Curr. Org. Chem.* **2006**, *10*, 491–518.
(5) (a) Malinovskii, V. L.; Wenger, D.; Haner, R. *Chem. Soc. Rev.* **2010**, *39*, 410–422. (b) Filichev, V. V.; Pedersen, E. B. 493−524. In *Wiley Encyclopedia of Chemical Biology*; Begley, T. P. , Ed.; Wiley-VCH Verlag GmbH & Co.: Weinheim, 2009. (c) Teo, Y. N.; James, N.; Wilson, J. N.; Kool, E. T. *J. Am. Chem. Soc.* **2009**, *131*, 3923–3933.
(6) Østergaard, M. E.; Hrdlicka, P. J. *Chem. Soc. Rev.* 2011, doi: 10.1039/C1CS15014F.
(7) (a) Koshkin, A. A.; Singh, S. K.; Nielsen, P.; Rajwanshi, V. K.; Kumar, R.; Meldgaard, M.; Olsen, C. E.; Wengel, J. *Tetrahedron* **1998**, *54*, 3607–3630. (b) Obika, S.; Uneda, T.; Sugimoto, T.; Nanbu, D.; Minami, T.; Doi, T.; Imanishi, T. *Bioorg. Med. Chem.* **2001**, *9*, 1001–1011. (c) Kaur, H.; Babu, B. R.; Maiti, S. *Chem. Rev.* **2007**, *107*, 4672–4697.
(8) Sørensen, M. D.; Kværnø, L.; Bryld, T.; Håkansson, A. E.; Verbeure, B.; Gaubert, G.; Herdewijn, P.; Wengel, J. *J. Am. Chem. Soc.* **2002**, *124*, 2164–2176.
(9) (a) Andersen, N. K.; Wengel, J.; Hrdlicka, P. J. *Nucleosides Nucleotides Nucleic Acids* **2007**, *26*, 1415–1417. (b) Kumar, T. S.; Madsen, A. S.; Østergaard, M. E.; Sau, S. P.; Wengel, J.; Hrdlicka, P. J. *J. Org. Chem.* **2009**, *74*, 1070–1081.
(10) Kumar, T. S.; Madsen, A. S.; Østergaard, M. E.; Wengel, J.; Hrdlicka, P. J. *J. Org. Chem.* **2008**, *73*, 7060–7066.
(11) Kumar, T. S.; Wengel, J.; Hrdlicka, P. J. *ChemBioChem* **2007**, *8*, 1122–1125.
(12) Sau, S. P.; Kumar, T. S.; Hrdlicka, P. J. *Org. Biomol. Chem.* **2010**, *8*, 2028–2036.
(13) Kumar, T. S.; Madsen, A. S.; Wengel, J.; Hrdlicka, P. J. *J. Org. Chem.* **2006**, *71*, 4188–4201.
(14) Yamana, K.; Iwase, R.; Furutani, S.; Tsuchida, H.; Zako, H.; Yamaoka, T.; Murakami., A. *Nucleic Acids Res.* **1999**, *27*, 2387–2392.
(15) Kalra, N.; Babu, B. R.; Parmar, V. S.; Wengel, J. *Org. Biomol. Chem.* **2004**, *2*, 2885–2887.
(16) Nakamura, M.; Fukunaga, Y.; Sasa, K.; Ohtoshi, Y.; Kanaori, K.; Hayashi, H.; Nakano, H.; Yamana, K. *Nucleic Acids Res.* **2005**, *33*, 5887–5895.
(17) Yamana, K.; Ohashi, Y.; Nunota, K.; Kitamura, M.; Nakano, H.; Sangen, O. S. *Tetrahedron Lett.* **1991**, *32*, 6347–6350.
(18) Oeda, Y.; Iijima, Y.; Taguchi, H.; Ohkubo, A.; Seio, K.; Sekine, M. *Org. Lett.* **2009**, *11*, 5582–5585.
(19) Sehgal, R. K.; Kumar, S. *Org. Prep. Proced. Int.* **1989**, *21*, 223–225.
(20) Prepared as described in: Roy, S. K.; Tang, J.-Y. *Org. Process Res. Dev.* **2000**, *4*, 170–171.
(21) Yamana, K.; Aota, R.; Nakano, H. *Tetrahedron Lett.* **1995**, *36*, 8427–8430.
(22) Zemlicka, J. *Collect. Czech. Chem. Commun.* **1964**, *29*, 1734–1735.
(23) Bair, K. W.; Tuttle, R. L.; Knick, V. C.; Corey, M.; Mc Kee, D. D. *J. Med. Chem.* **1990**, *33*, 2385–2393.
(24) (a) Dale, T. J.; Rebek, J. *J. Am. Chem. Soc.* **1990**, *33*, 2385–2393. (b) Asseline, E.; Cheng, E. *Tetrahedron Lett.* **2001**, *42*, 9005–9010.
(25) Disappearance of $^{1}$H NMR signals from exchangeable protons upon $D_2O$ addition, in concert with NMR ($^{1}$H, $^{13}$C, COSY, and HSQC) and HRMS, ascertained the O2′/N2′-functionalized constitution of the reported nucleosides.
(26) Ross, B. S.; Springer, R. H.; Tortorici, Z.; Dimock, S. *Nucleosides Nucleotides* **1997**, *16*, 1641–1643.
(27) Al-Rawi, S.; Ahlborn, C.; Richert, C. *Org. Lett.* **2005**, *7*, 1569–1572.
(28) Abdel-Magid, A. F.; Carson, K. G.; Harris, B. D.; Maryanoff, C. A.; Shah, R. D. *J. Org. Chem.* **1996**, *61*, 3849–3862.
(29) Sanghvi, Y. S.; Hoke, G. D.; Freier, S. M.; Zounes, M. C.; Gonzalez, C.; Cummins, L.; Sasmor, H.; Cook, P. D. *Nucleic Acids Res.* **1993**, *21*, 3197–3203.
(30) Guckian, K. M.; Schweitzer, B. A.; Ren, R. X.-F.; Sheils, C. J.; Tahmassebi, D. C.; Kool, E. T. *J. Am. Chem. Soc.* **2000**, *122*, 2213–2222.
(31) (a) Printz, M.; Richert, C. *J. Comb. Chem.* **2007**, *9*, 306–320. (b) Printz, M.; Richert, C. *Chem.—Eur. J.* **2009**, *15*, 3390–3402.
(32) Christensen, U. B.; Pedersen, E. B. *Nucleic Acids Res.* **2002**, *30*, 4918–4925.
(33) Bryld, T.; Højland, T.; Wengel, J. *Chem. Commun.* **2004**, 1064–1065.
(34) Hendrix, C.; Devreese, B.; Rozenski, J.; van Aerschot, A.; de Bruyn, A.; van Beeumen, J.; Herdewijn, P. *Nucleic Acids Res.* **1995**, *23*, 51–57.
(35) Karla, N.; Parlato, M. C.; Parmar, V. S.; Wengel, J. *Bioorg. Med. Chem. Lett.* **2006**, *16*, 3166–3169.
(36) Korshun, V. A.; Stetsenko, D. A.; Gait, M. J. *J. Chem. Soc., Perkin Trans. 1* **2002**, 1092–1104.
(37) Dohno, C.; Saito, I. *ChemBioChem* **2005**, *6*, 1075–1081.

(38) Dougherty, G.; Pilbrow, J. R. *Int. J. Biochem.* **1984**, *16*, 1179–1192.
(39) Manoharan, M.; Tivel, K. L.; Zhao, M.; Nafisi, K.; Netzel, T. L. *J. Phys. Chem.* **1995**, *99*, 17461–17472.
(40) Nakano, S.-I.; Uotani, Y.; Uenishi, K.; Fujii, M.; Sugimoto, N. *J. Am. Chem. Soc.* **2005**, *127*, 518–519.
(41) Benvin, A. L.; Creeger, Y.; Fisher, G. W.; Ballou, B.; Wagonner, A. S.; Armitage, B. A. *J. Am. Chem. Soc.* **2007**, *129*, 2025–2034.
(42) Nakamura, M.; Murakami, Y.; Sasa, K.; Hayashi, H.; Yamana, K. *J. Am. Chem. Soc.* **2008**, *130*, 6904–6905.
(43) Sekine, M.; Oeda, Y.; Iijima, Y.; Taguchi, H.; Ohkubo, A.; Seio, K. *Org. Biomol. Chem.* **2011**, *9*, 210–218.
(44) Gupta, P.; Langkjaer, N.; Wengel, J. *Bioconjugate Chem.* **2010**, *21*, 513–520.